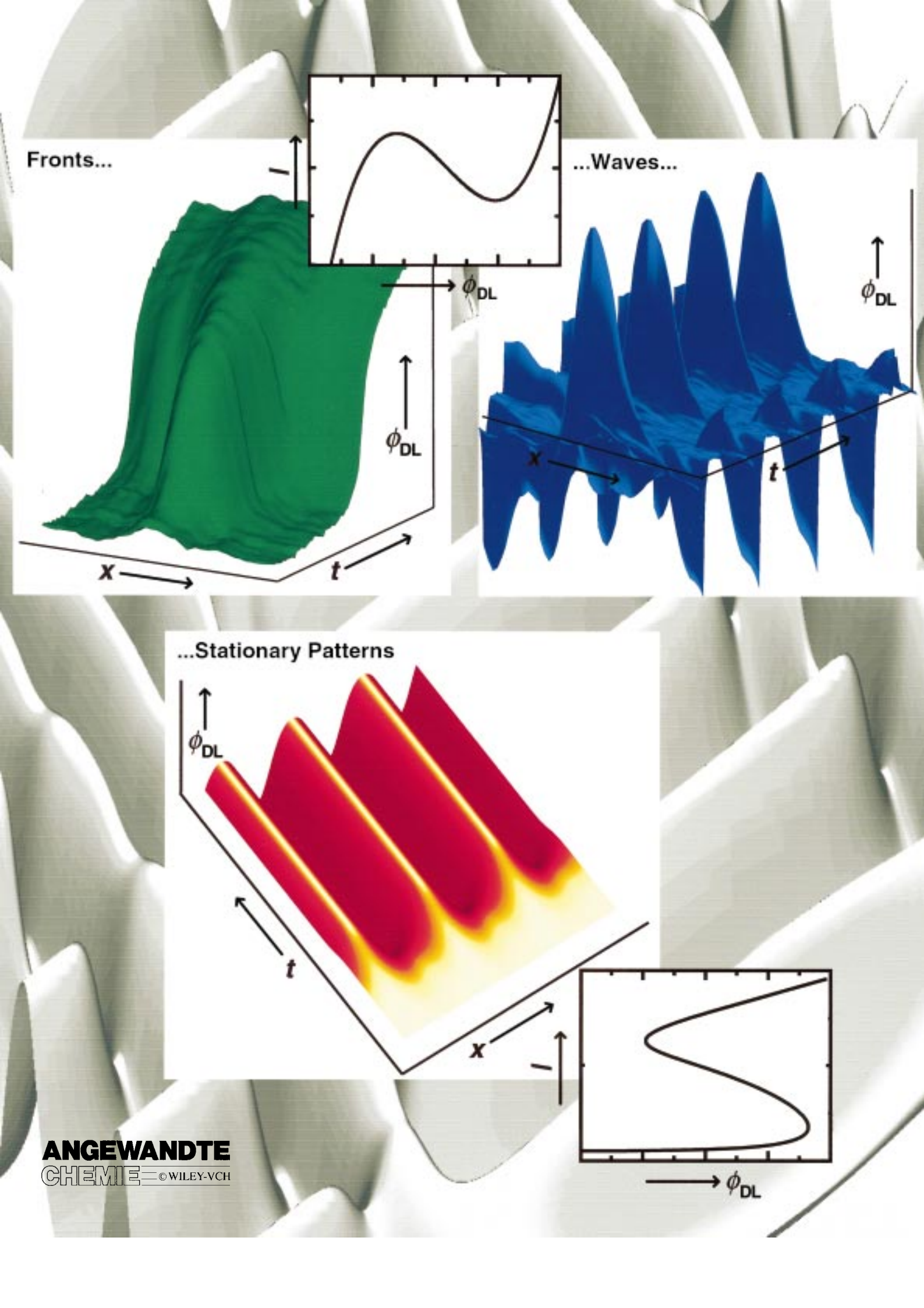

ANGEWANDTE CHEMIE

Fronts, Waves, and Stationary Patterns in Electrochemical Systems**

Katharina Krischer,* Nadia Mazouz, and Peter Grauel

Oscillatory behavior has been observed for almost all electrochemical reactions in a certain, although sometimes small, range of external parameters. Only in the past ten years has it been possible, however, to find a common explanation for the occurrence of these temporal self-organization phenomena of chemically completely different electrochemical reactions. The breakthrough was achieved because new methods and concepts, which had been developed in nonlinear dynamics to describe the spontaneous formation of order in various disciplines, could be applied. This development in turn was only possible because the underlying laws are universal at a certain abstract level. Oscillations are only one possible manifestation of nonlinear behavior. Examples of other features that are often closely associated with temporal instabilities are spatial structures and waves. Initiated by the theoretical progress and the development of new experimental techniques, spatial pattern formation in electrochemical systems has been targeted for investigations in the past few years. Based on these investigations, it can be predicted under which conditions temporal or spatial pattern formation can be expected. Furthermore, the possibility of predicting the occurrence of instabilities indicates that it might be feasible to exploit nonlinear effects to increase, for example, the yield of electrocatalytic reactions. Here we discuss physicochemical mechanisms that lead to pattern formation in electrochemical systems. At the same time, we stress the generic principles that are responsible for self-structuring processes in many chemical and biological systems.

Keywords: autocatalysis · electrochemistry · nonlinear dynamics · pattern formation · self-organization

1. Introduction

> *I would like to hold off on any comment on my beliefs about the cause of these strange appearances until an experimental basis can be offered to you.*[1]
> Wilhelm Ostwald, 1900

A system far from thermodynamic equilibrium can spontaneously form a state of higher order if the evolution equations of the system are nonlinear and fulfill certain requirements.[2] This knowledge led to a new understanding of many natural phenomena in the second half of the 20th century. For example, a metal wire that spontaneously forms a hot and a cold zone cannot be explained in classical thermodynamics. However, this very phenomenon can be observed when the wire catalyzes a chemical reaction and the average temperature of the wire is kept constant.[3, 4] As a result of the composition of the reactants and the control of the temperature the system is far from equilibrium. The evolution equations for the local temperature and the local activity of the wire contain appropriate terms. Both the nonequilibrium condition and the nonlinear evolution equation enable an export of entropy out of the system, and results in a state of higher order within the system. A process that results in a state of higher order in a system by exporting entropy out of it is called a self-organization process. Examples of self-organization can be found in all the natural sciences. Conditions under which order can develop on mesoscopic and macroscopic scales are at the center of nonlinear dynamics.

One of the main findings of the theory of nonlinear systems is that complex motion or structures can originate from the interaction of a few variables rather than through the linear superposition of many degrees of freedom. In this context, the occurrence of deterministic chaos is certainly the most spectacular feature. It is also responsible for the limited predictability of the dynamics of macroscopic systems. Furthermore, results from various scientific disciplines have shown that mechanisms leading to the occurrence of nonequilibrium structures are universal. The same fundamental laws are responsible for the periodic rhythms in "chemical

[*] Priv.-Doz. Dr. K. Krischer, Dr. N. Mazouz, Dr. P. Grauel
Fritz-Haber-Institut der Max-Planck-Gesellschaft
Faradayweg 4–6, 14195 Berlin (Germany)
Fax: (+49)30-8413-5106
E-mail: Krischer@fhi-berlin.mpg.de

[**] In the appendix we list the minimal equations (prototype equations) that describe the phenomena of self-organization discussed in the individual sections.

  1433-7851/01/4005-0851 $ 17.50+.50/0

clocks", many biological systems, some semiconductors and lasers, and the electrochemical systems described here. Thus, this overview of electrochemical self-organization can be looked at from an interdisciplinary point of view as well. On a certain abstract level, the basic principles can be applied to many systems that are fundamentally different in nature, especially to chemical pattern-forming systems.

If we look at the mechanism that results in instabilities from the point of view of physical chemistry, it is already clear by glancing at the history of chemical oscillations that electrochemical reactions need to have a special feature that favors the occurrence of instabilities. The first electrochemical oscillations were described in the 1820s, more than 100 years before those of other chemical systems.[5] Today, the number of known electrochemical systems displaying self-organization is greater by far than that of chemical oscillators in homogeneous phases (many have been listed in review articles[6–8]).

The most famous example is the electrooxidation of metals, above all, that of iron, which has been investigated as a chemical model for nerve impulse propagation at the beginning of the 20th century.[9, 10] Deposition of metals is also often connected with oscillations of the reaction rate. The same applies to apparently simple oxidation and reduction reactions, such as the oxidation of Fe^{2+}, iodide, or hydrogen or the reduction of peroxodisulfate, iodate, or periodate. Furthermore, electrocatalytic reactions exhibit dynamic instabilities, which start with the oxidation of formic acid, formaldehyde, and methanol, continue with members of their respective homologous series, and end with the reduction of hydrogen peroxide and oxygen.

In contrast to chemical reactions performed in a homogeneous phase under isothermal conditions, almost all electrochemical reactions are observed to have oscillating behavior in a certain range of the external parameters (for example, voltage or bulk concentrations of the reactants). The frequent occurrences of phenomena of self-organization are widespread in electrochemical reactions, which explains the long history of these chemical oscillators. It also shows how important it is to understand the physicochemical origins of these occurrences in chemically completely different reactions. It has not yet been ten years since a general explanation, based on some previous research, was given for temporal instabilities of electrochemical oscillators.[11] A general mathematical model for spatial pattern formation was formulated about five years ago.[12] This gain in understanding led to a new wave of experimental investigations, which in turn brought to light a variety of spatiotemporal phenomena at the electrode/electrolyte interface.

As is the case for electrochemical pattern formation, chemical oscillators presented in this review can be described by so-called reaction–transport equations.[13] The term "reaction" stands for the dynamic of the system in the absence of any spatial inhomogeneities, that is, for the homogeneous system. The "transport" term plays a role only when spatial variations are present in the variables parallel to the spatial domain, which in our case is the electrode.

As a necessary prerequisite for the formation of spatial patterns, the reaction part (that is, the homogeneous dynamic) has to have a certain structure that often results in temporal instabilities such as bistable or oscillatory behavior.[14] Thus,


K. Krischer


N. Mazouz


P. Grauel

Katharina Krischer studied Chemistry in Berlin and Munich. She obtained her PhD in 1990 from the Free University (FU), Berlin, with Professor Ertl. After that, she was a postdoctoral fellow in the Department of Chemical Engineering at Princeton University, NJ, USA, working on theoretical studies of structure-forming processes. Subsequently, she returned as a principal investigator to the Fritz-Haber-Institute of the Max-Planck-Gesellscaft (MPG), Berlin. Since then her studies have focused on spatiotemporal pattern formation in electrochemical systems. In 1998 she obtained her Habilitation from the FU, Berlin, and became a lecturer in Physical Chemistry. She was honored with the Otto Hahn Medal of the MPG, the ADUC annual award (ADUC Jahrespreis für Habilitanden), and the de Gruyters Award of the Berlin-Brandenburg Academy of Sciences. Her research interests include all overlapping aspects of electrochemistry and nonlinear dynamics.

Nadia Mazouz studied Physics and Philosophy in Berlin. Having obtained her Diplom in Physics from the Technical University (TU), Berlin, in 1996, she worked on theoretical studies of self-organization processes of electrode reactions at the Fritz-Haber-Institute, Berlin. She obtained her PhD on the same studies in 1999 from the FU, Berlin. Since then, aside from the theory of complex systems, her studies have intensified again on philosophical questions.

Peter Grauel graduated in Chemistry from the University of Frankfurt in 1995. He then worked on experimental studies of interfaces and studies of electrochemical structure formation processes at the Fritz-Haber-Institute, Berlin. He obtained his PhD from the FU Berlin in 1999, and has since been working as a scientific researcher at the Fritz-Haber-Institute.

spatial pattern formation is the result of the interaction of a homogeneous dynamic and lateral transport processes.

The transport process connected to pattern formation in chemical systems is essentially always diffusion. Chemical systems, especially the Belousov–Zhabotinsky reaction, are considered prototypes of pattern-forming systems and model systems for biological systems. Thus, most theoretical studies on pattern formation in reaction–transport systems concentrate on pattern formations in reaction–diffusion systems. As we will discuss, the dominant spatial coupling in electrochemical systems results from changes of the electric field in the electrolyte. This coupling differs from the diffusion coupling in some aspects, and can lead to qualitative new behavior in pattern formation.

This review gives an overview on the latest developments in electrochemical processes of self-organization. Section 2 covers systems whose behavior can be described by spatiotemporal changes in the double-layer potential alone, the central variable in electrochemistry. We will show that the double-layer potential behaves autocatalytically in these systems. We expand our presentation in Section 3 to situations where the dynamic behavior is influenced not only by an autocatalytic double-layer potential but also by an additional—chemical—variable, namely a concentration or a coverage of the electrode. The feedback of this additional variable onto the temporal development of the double-layer potential results in oscillating behavior that is the key characteristic of all features presented in this section. Subsection 3.1 deals with more complex forms of oscillations that are displayed when the system has an additional feedback loop. Finally, Section 4 describes systems in which the roles of the chemical variable and the double-layer potential are reversed with respect to those discussed in Section 3. Section 5 summarizes the characteristics of pattern formation in electrochemical systems and discusses future perspectives.

The three main Sections 2–4 have the same setup. First, the homogeneous system is presented, then the influence of transport processes parallel to the electrode is taken into account, and finally, the influence of an external control of the reaction on pattern formation is discussed. Such a control of the reaction could occur if the total current is kept constant, for example.

2. Fronts in Bistable Systems

The simplest nontrivial behavior of a nonlinear system is bistability, whereby two stable, stationary and spatially homogeneous states coexist in a certain range of the experimental parameters.[14, 15] These states are stable with respect to sufficiently small perturbations. For larger perturbations, the system can show transitions from one state to the other. The transitions are normally not homogeneous, that is, they do not occur at all locations of the system at the same time. Rather, they are associated with the formation and propagation of fronts: narrow, propagating regions that connect the areas of the system that are in different states.

2.1. Homogeneous Dynamic

The occurrence of bistable behavior in electrochemical systems is closely associated with the operational mode of the experiment. A standard setup of an electrochemical experiment is shown in Figure 1a. Investigations focus on the interface

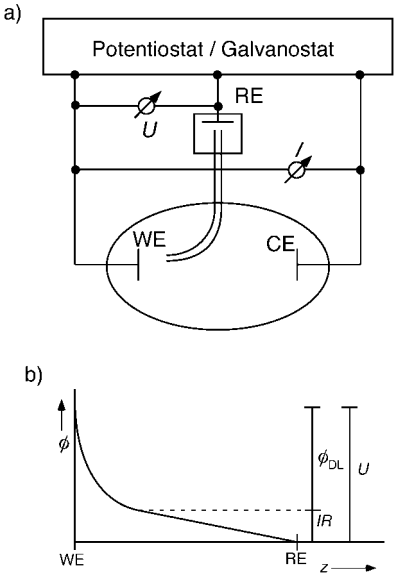

Figure 1. a) Basic electrochemical experimental setup. WE: working electrode, CE: counter electrode, RE: reference electrode. The reference electrode is in a separate compartment, and is connected to the actual electrochemical cell by a electrolyte bridge (Luggin capillary). b) Distribution of the voltage drop between the working electrode and the reference electrode in terms of the voltage drop across the double layer ϕ_{DL} and the Ohmic (IR) drop in the electrolyte. z is the spatial direction perpendicular to the electrode.

between the working electrode (WE) and an electrolyte. If a current flows through this interface, the second transition, from an ionic conductor to an electronic conductor, takes place at the counter electrode (CE). The potential of the working electrode is measured with respect to a third electrode with constant potential: the reference electrode (RE). The potential drop between the working electrode and the reference electrode is composed of the potential drop across the double layer (ϕ_{DL}, subsequently called electrode potential or double-layer potential) and the Ohmic drop in the electrolyte (Figure 1b). For the potentiostatic operational mode, the voltage U between the working electrode and the reference electrode is controlled by a potentiostat, and the current is measured. For galvanostatic experiments, the total current flowing through the cell is kept constant and the voltage is measured between the working electrode and the reference electrode.

If the Ohmic drop in the electrolyte between the working electrode and the reference electrode cannot be neglected, the current–electrode potential (I/ϕ_{DL}) relationship, which is the curve of interest, differs significantly, sometimes qualitatively, from the measured current–voltage (I-U) relationship. In the 1960s it was already evident that an N-shaped dependence of the reaction current on the double-layer potential (Figure 2a) can lead to bistable behavior in the

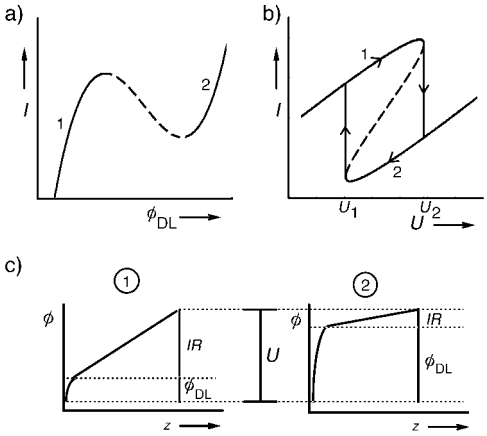

Figure 2. a) N-shaped current versus electrode potential relationship. The NDR range is depicted as a dashed line. b) Bistable current – voltage curve. c) Distribution of the applied voltage in terms of the electrode potential and the potential drop in the electrolyte for the two coexisting stable states.

current – voltage relationship if the cell resistance exceeds a threshold value (Figure 2b): Three combinations of double-layer potential and Ohmic voltage drop exist in a certain range of the external voltages. For these combinations, the potentiostatic control condition $U = \phi_{DL} + IR$, is met. The state corresponding to the medium current value is then on the negative differential branch of the I/ϕ_{DL} curve and is unstable, which means it cannot be realized experimentally. The two stable stationary states are at branches 1 and 2 of the I/ϕ_{DL} curve, where it has a positive slope (Figure 2c).

The instability is the result of the interaction between the negative differential resistance (NDR) of the I/ϕ_{DL} relationship and the potentiostatic mode of operation. Imagine the system takes a state on the NDR branch (dashed line in Figure 2a). In this case, a small perturbation of ϕ_{DL} to somewhat higher values then results in a decrease in the stationary current and, therefore, in a decreased IR drop in the electrolyte. If the decrease in the IR drop is larger than the increase in the double-layer potential arising from the fluctuation then $\phi_{DL} + IR < U$. The working electrode is thus instantly charged (because of a feedback of the potentiostat) and ϕ_{DL} is pushed to even more positive values. However, at the more positive value of ϕ_{DL} the reaction current is even smaller, such that the described process is enhanced until a state is reached on the outer branch with positive slope (2). The control condition is met in this state, and it is stable with respect to small fluctuations.

Analogous to this, the system reaches a state on the external branch with low potentials (1) if ϕ_{DL} decreases as a consequence of the initial fluctuation. Thus, a small perturbation of the stationary state on the NDR branch is enhanced. As with autocatalytic reactions, the temporal change of the double-layer potential is proportional to its actual value upon linear approximation, whereby the proportionality constant is positive. Thus, ϕ_{DL} is an autocatalytic variable here.

Bistability in a homogeneous system is essentially always connected to autocatalysis, and is independent of the type of system. Therefore, all chemical systems that display bistability have a reaction step in which an intermediate enhances its own production.[16] Thus temperature can take on the function of the self-enhancing variable in exothermic, homogeneously or heterogeneously catalyzed reactions.[17] The temporal evolution of the potential drop at an interface in many semiconductors[18] or membranes[19] is responsible for the positive feedback, a process that is analogous to the electrochemical systems described above.

Dynamic instabilities are often found in electrochemical systems because of the ease with which a negative differential resistance forms.[11] It occurs, for example, if the surface of the electrode becomes chemically altered because of a change in the electrode potential in the direction of higher overpotential such that the rate of the electrochemical reaction is reduced. This is the case for the best known electrochemical oscillators, the metal dissolution reactions, where the oxidation rate of the metal is reduced or even fully inhibited because an oxide layer forms. Other causes for the formation of a negative differential resistance can be adsorption of a nonreactive species dissolved in the electrolyte, such as an ion of the conducting salt. In addition, electrostatic interactions with charged reactants or the potential-dependent desorption of a catalyst can result in a negative differential resistance.

Three experimental examples of bistable I/U plots are depicted in Figure 3. Figure 3a shows a cyclic voltammogram of the reduction of peroxodisulfate at an Ag electrode. For this system, the negative differential resistance responsible for

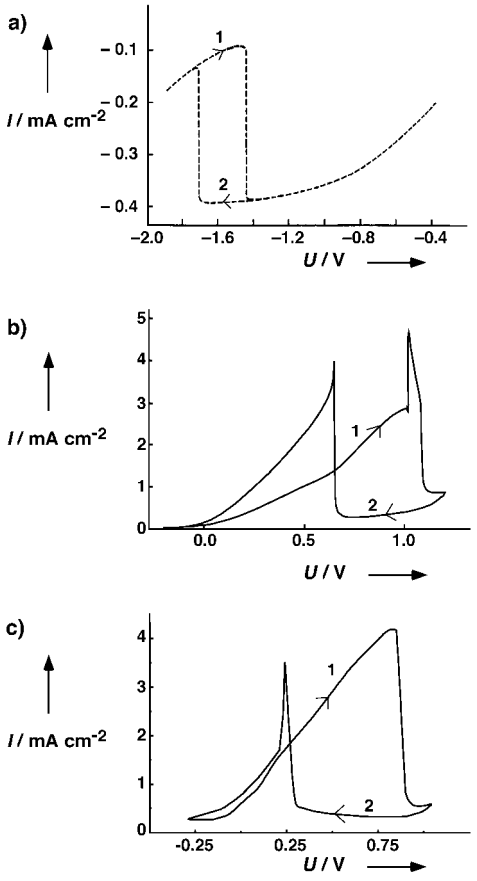

Figure 3. Experimental examples of bistable current – voltage curves: a) reduction of $S_2O_8^{2-}$ on Ag; b) oxidation of H_2 in the presence of Cu^{2+} and Cl^- ions on Pt; c) formic acid oxidation on Pt. U is given versus the SCE. (Figure 2c was generously provided by P. Strasser; see also ref. [77]).

the bistability arises from the electrostatic repulsion of the peroxodisulfate ions at potentials at which the electrode is negatively charged.[20] Figure 3b shows the current–voltage curve of hydrogen oxidation on a Pt electrode in the presence of Cu^{2+} and Cl^- ions. Here, the adsorption of chloride ions results in a decrease in the oxidation current of the active branch 1 at about 1.2 V. As a consequence, the double-layer potential increases and reaches a range where formation of PtOH takes place. This results in an inactive electrode (branch 2). (The current peak just before the transition to the inactive branch is caused by the interaction between Cu and chloride ions on adsorption.[21])

Negative differential resistance and, thus, bistability during the oxidation of formic acid (Figure 3c) are also caused by the formation of a nonreactive PtOH electrode. Besides the electrooxidation of iron, cobalt, or nickel, the three systems listed above are the ones whose spatiotemporal behavior has been most investigated. Therefore, we will run into these systems time and again in this review.

2.2. Accelerated Fronts by Nonlocal Migration Coupling

A local perturbation or a fluctuation in a homogeneous stationary state triggers a front if the perturbation has a critical size and passes a threshold value.[14, 15] The motion of the front, as well as the occurrence of all other patterns discussed here, arise because of the interaction of the homogeneous system dynamic and lateral transport processes. For a bistable case, this can be visualized with a simple schematic (Figure 4): Imagine a bistable system being partly

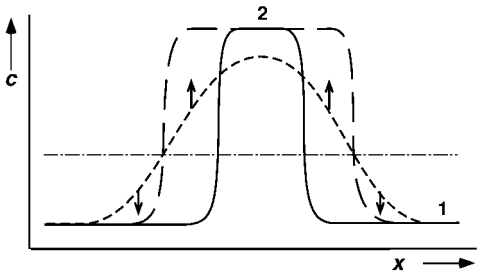

Figure 4. Development of a front in bistable media by interaction of an autocatalytic reaction and a transport process.

in one of the two stable states and partly in the other state (solid line). A gradient in the autocatalytic variable then exists in the transition region of the two states. If we assume that this is a concentration then the concentration gradient leads to a particle flux, which would result in an adjustment of the concentration difference without the autocatalytic reaction step. Thus, diffusion causes a lateral expansion of the transition range (line with short dashes). However, the autocatalytic kinetic acts against this homogenizing process: Autocatalysis causes all ranges in which the concentration is above a certain threshold (the unstable stationary state, dotted line with dashes) to evolve toward stationary state 2. All ranges below this threshold evolve toward state 1 (arrows). These processes, which actually take place simultaneously, result in the propagation of the transition range, that is, in a front: The more stable of the two states (state 2 in Figure 4) expands while the region of the metastable state decreases (line with long dashes). Moreover, the front profile and the propagation velocity remain constant. Both are determined by the parameters of the system, which normally are rate constants and diffusion constants.[14, 15]

In electrochemical systems with N-shaped current versus double-layer potential curves, the double-layer potential ϕ_{DL} is the central and autocatalytic variable. Accordingly, the fronts are potential fronts. An inhomogeneous potential distribution of ϕ_{DL} affects the distribution of the potential in the whole electrolyte. The potential distribution in the electrolyte is determined by the electroneutrality of the electrolyte. Therefore, a change in the distribution of the double layer potential also changes the migration currents at the electrode/electrolyte interface.[22] These changes cause a position-dependent recharging of the double layer. They are thus responsible for the occurrence of fronts in bistable systems. Hence, the patterns arise as a result of the interaction of the migration and the dynamic of the homogeneous system described in Section 2.1. The manifestation of the reaction–migration fronts, however, normally differs from the typical reaction–diffusion fronts. The variation in the reaction–migration fronts is bigger than that of reaction–diffusion fronts. This can be seen when experimental examples are compared (Figure 5).

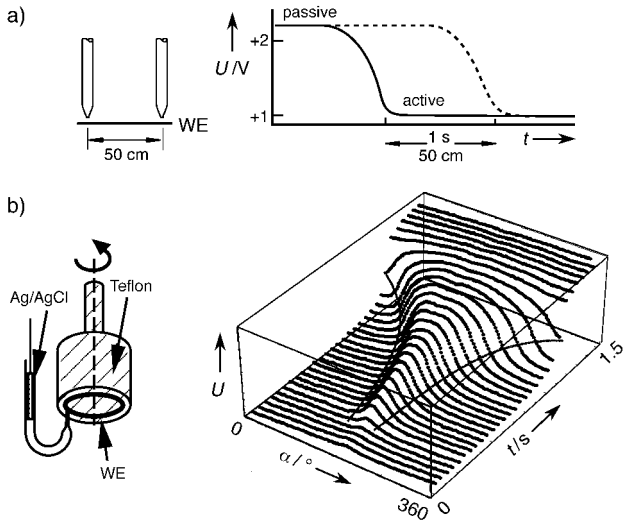

Figure 5. Experimental potential fronts a) during the corrosion of gold in a concentrated HCl/NaCl solution (according to ref. [23]), b) during the potentiostatic reduction of $S_2O_8^{2-}$ on an Ag ring electrode in dilute electrolyte.[22] On the left are the corresponding experimental setups.

Figure 5a shows plots of potential versus time for the electrodissolution of gold at two positions of a wire 50 cm apart.[23] The large drop in the electrode potential by more than 1 V is the result of a passing passive front. This front passes the second potential probe one second later. Both curves are of an identical shape, which implies there is a constant front profile as well as a constant velocity.

In contrast, an increase in the velocity with which the potential fronts propagate across the electrode can be seen clearly in the temporal evolution of potential profiles (Fig-

ure 5b, right). These potential profiles were recorded in front of a ring electrode during the reduction of peroxodisulfate.[22] The spatial resolution was obtained with a single measuring probe over which the ring electrode was rotated (Figure 5b, left). The rotation of the ring electrode further ensures a defined mass transport. Accelerated fronts of the potential have since been found for several systems such as for cobalt[24] and iron dissolution.[25, 26]

The different propagation behavior of electrochemical fronts compared to fronts in reaction–diffusion systems is a consequence of a different range of spatial coupling.[12, 27] As mentioned above, the coupling of the electrode to the electrolyte plays the most important role for the spatial coupling in electrochemical systems: An inhomogeneous distribution of double-layer potential also induces a potential pattern in the electrolyte. This potential pattern adjusts itself such that the electrolyte (outside of the double layer) always stays electroneutral. The potential pattern reaches up to the counter electrode, and hence we can assume that an equipotential plane exists in front of the counter electrode. The amplitude of the potential pattern in the electrolyte decreases with increasing distance from the electrode and expands parallel to the electrode at the same time (Figure 6a, top). The expansion is also felt at the electrode/electrolyte interface in the form of changed migration current densities. Intuitively it becomes clear that the migration coupling encompasses a wide range of the electrode, sometimes even all of the interface. This situation is illustrated in the bottom portion of Figure 6a. The length of the arrows indicates schematically the instantaneous contribution of migration coupling to the recharging of the double layer. Spatial coupling in electrochemical systems is therefore long-range or nonlocal: A perturbation of the state of the electrode at a certain location x_0 instantaneously causes a change of states at locations far away from the disturbance. The closer a given location is to x_0, the larger the change at this location.

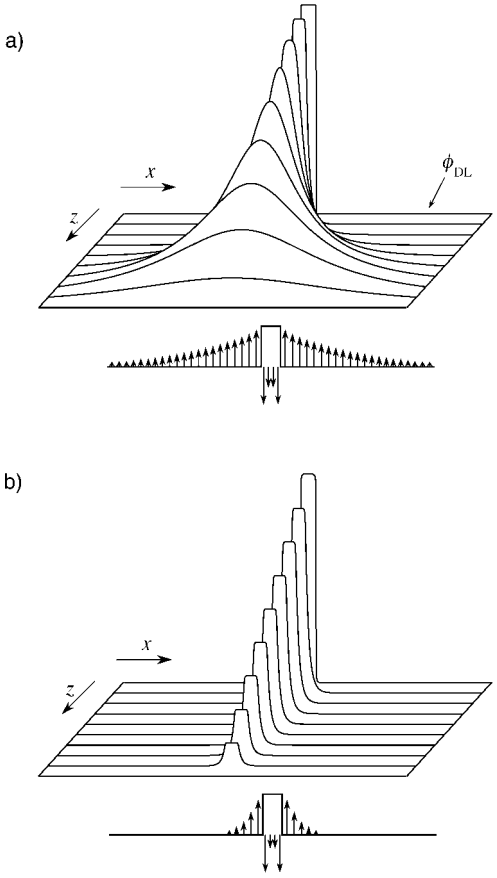

Figure 6. Schematic representation of the potential distribution in the electrolyte as a result of an inhomogeneous distribution of the electrode potential ϕ_{DL}, and the effect of migration currents induced by the inhomogeneous potential distribution on the local temporal evolution of the potential a) for the case that the ratio of the distance WE/CE to the length of WE is >1, b) for the case that this ratio is $\ll 1$. (x, z: spatial coordinates parallel and perpendicular to the electrode, respectively. The electrode is assumed to be one-dimensional and the electrolyte two-dimensional.)

The range of the migration coupling depends on the ratio of the size of the working electrode (the length of the electrode for an essentially one-dimensional electrode or the circumference for a ring electrode) to that of the distance between the working electrode and the equipotential plane, normally the counter electrode. The closer the counter electrode and working electrode are, the less noticeable is the expansion of the potential pattern parallel to the working electrode (Figure 6b, top). This leads to a smaller range of the spatial coupling (Figure 6b, bottom). In the limit of vanishing distances between working electrode and counter electrode, the nonlocal coupling changes to a nearest-neighbor coupling or local coupling, in which only an infinitely small environment immediately feels a noticeable contribution of the spatial coupling.[12, 27] This is also the situation seen with diffusive coupling. In this sense, diffusion coupling is a local coupling.[14]

The nonlocal coupling is the reason why electrochemical fronts usually do not propagate with constant but with increasing velocity.[27] The motion of the front is therefore accelerated if the distance between the working electrode and counter electrode is large. This situation applies to most experimental setups and was also the case for the measurements presented in Figure 5b. At the time the measurements shown in Figure 5a were carried out the connection between cell geometry and propagation behavior of fronts was not yet known, and the relative location of the electrodes can unfortunately no longer be reconstructed. However, since a wire of more than 50 cm in length was used as a working electrode in the experiment, it is likely that the ratio of the distance between the working and counter electrode (or the equipotential plane parallel to the working electrode) relative to the length of the electrode was $\ll 1$. Thus, conditions probably existed in which the migration coupling can be approached by a diffusion coupling.

2.3. Control of Front Speed by Global Coupling

Aside from local or nonlocal coupling, global coupling also often exists in chemical and physical systems, especially if one variable is subject to external control. Global coupling means that the change of the state at a particular location is instantly and equally affected by a certain change of the state at any arbitrary location. In the last few years it has been demonstrated by theoretical investigations as well as by experiments

that global coupling in different dynamic situations can have an enormous effect on the spatiotemporal dynamic of a system, such as for heterogeneously catalyzed reactions, for semiconductors that were particularly similar to electrochemical systems[28, 29], or for gas discharge systems.[30]

Individual locations of the electrode can be coupled globally in electrochemical experiments by the potentiostatic as well as the galvanostatic mode of operation.[31–34] The explanation for this may be obvious for galvanostatic systems: If the current density changes at a particular location, the total current changes. As soon as the latter differs from the set current, the galvanostat varies the potential of the electrode. This variation immediately leads to a change in the potential drop across the double layer at all locations of the electrode, and, thus, to a global coupling of the individual locations of the electrode. For the potentiostatic mode of operation, the global coupling becomes important if the reference electrode is close to the working electrode. This can be understood better if one recalls that a local change of the double-layer potential changes the potential distribution in all of the electrolyte. This change is bigger at the working electrode than farther away from it. Consequently, if the reference electrode is close to the working electrode, a local change of the double-layer potential causes the set voltage between the reference and the working electrode to differ from the actual voltage. Therefore, the change causes the potentiostat to vary the potential of the working electrode. This scenario is analogous to the galvanostatic case, and the result is a change of the double-layer potential along all of the electrode.

Here we should mention that we implicitly assumed that the reference electrode is far away from the working electrode in the examples in Section 2.2. Thus, the above-mentioned global coupling does not influence the dynamic in the examples. The front behavior changes qualitatively if global coupling is present, as we will discuss below.

For global coupling, the temporal evolution of a local state depends generally on the spatial mean of a variable. In the case of electrochemical systems, the partial differential equation for the dynamic of the double-layer potential contains a term of the form $\alpha\langle\phi_{DL}\rangle$, where the brackets symbolize that the average is formed. α is a parameter that is dependent on various system parameters such as the specific conductivity of the electrolyte and displays the strength of the global coupling (see Appendix). It can be seen from the corresponding equivalent circuits that the sign of α is positive under galvanostatic control[34] and negative under potentiostatic control for a close reference electrode.[31] Thus, one speaks of positive and negative global coupling.

The sign of the global coupling influences the effect of the coupling. Again, this can best be shown for a transition in the bistable regime. The starting point for our considerations is the situation depicted in Figure 4, that is, a bistable system in which a small range underwent a transition from the original homogeneous state 1 to state 2. If state 2 has the larger value of the double-layer potential, the nucleation of state 2 results in a larger mean value $\langle\phi_{DL}\rangle$. As a consequence, all locations originally in state 1 experience a change in the direction of larger values of ϕ_{DL} for positive global coupling. This leads state 1 to drift to larger values. However, above all, the transition from state 1 to state 2 is accelerated close to the front since a broader range is lifted above the threshold value as a result of the concerted action of migration coupling and global coupling. The self-accelerating effect of the transition can be seen: In the next time step the mean value increases further as does the speed with which the locations close to the front skip to state 2. In extreme cases, namely, for very big values of α, this leads to an essentially homogeneous transition whereby practically the whole electrode is driven to state 2 after its nucleation. Overall then, we note that the front acceleration is enhanced for positive global coupling.

For negative global coupling everything is reversed: When state 2 nucleates, positions in state 1 are driven to smaller values of ϕ_{DL}, that is, farther away from state 2. Accordingly, the effect of the migration coupling, which is still present, is reduced in the transition region of states 1 and 2. Without global coupling its interaction with the homogeneous dynamic would result in the propagation of state 2. Thus, the propagation speed of the front is reduced in the presence of a negative global coupling. Beyond a threshold of the coupling strength $|\alpha|$, the velocity of the front can become zero. In that case a stationary dissipative structure arises: Two ranges with different ϕ_{DL} coexist on the electrode. Figure 7 shows two experimental examples of stationary domains of the potential that formed spontaneously when a close reference electrode was used. At the bottom of the figure the corresponding current–voltage plots are presented. The arrow indicates the value of the voltage for which the spatiotemporal data were obtained.

The data of Figure 7a were measured during the reduction of $S_2O_8^{2-}$ at an Ag ring electrode with the same experimental setup as the accelerated fronts of the potential depicted in Figure 5b (except for a closer reference electrode).[31] The effect of the position of the reference electrode on the front behavior is particularly impressive when these two figures are compared. Figure 7b shows data obtained during the oxidation of H_2 at a Pt electrode in the presence of Cu^{2+} and Cl^- ions. A rotating ring electrode was used in this experiment as well, and the spatiotemporal data were measured with a setup analogous to that shown in Figure 5b. In addition, one can see in Figure 7b how the corresponding domains evolve from a homogeneous state after the external voltage has been set. The formation of the potential domains was observed for both systems in the voltage range in which the transition between the branches with high and low current density takes place. The ratio of the size of the two domains changes continuously if U is varied in this range.[31, 35]

The experiment depicted in Figure 8a shows very clearly the effective influence of synchronizing migration coupling and negative global coupling. The data were obtained during the oxidation of formic acid at a stationary Pt ring electrode in the bistable regime of the reaction using a close reference electrode.[36] The local potential was measured in this experiment with the help of 11 stationary potential probes. These probes were placed, together with a trigger electrode at position 12, over the ring electrode (Figure 8b). The double-layer potential was pushed further into the passive range at the locations marked by arrows (the ring position 12 $\hat{=}$ 0) by a pulse produced with the trigger electrode at time 0. This caused a transition to the active state at the 180° position, that

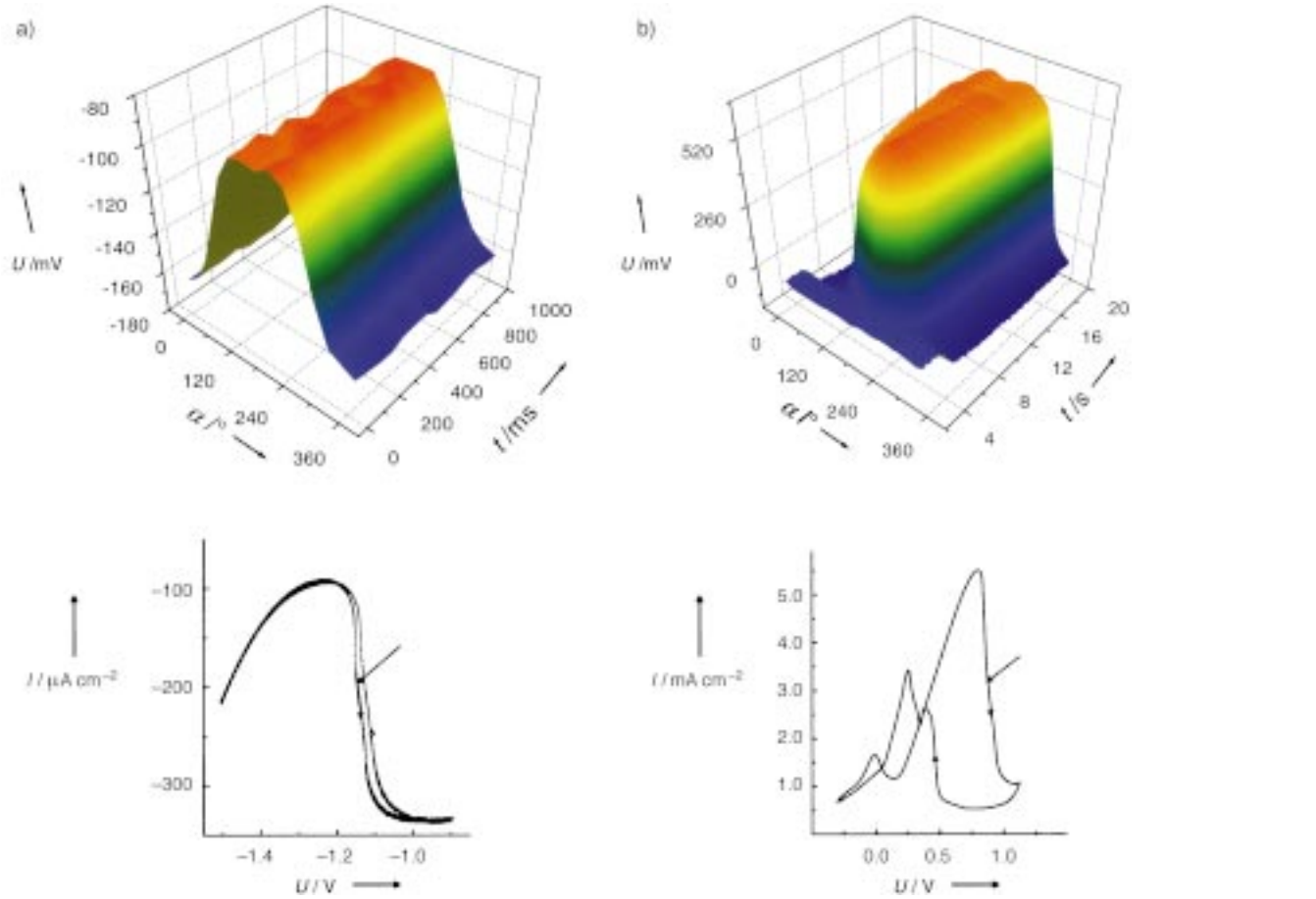

Figure 7. Stationary potential domains measured with a Haber–Luggin capillary (that is, a centric RE close to the WE) a) for the potentiostatic reduction of $S_2O_8^{2-}$ on an Ag ring electrode,[31] b) for the potentiostatic oxidation of H_2 on Pt in the presence of Cu^{2+} and Cl^- ions. At the bottom are the corresponding cyclic voltammograms obtained for this electrode arrangement. The arrows indicate the values of the voltage for which spatiotemporal data were obtained (in stationary measurements). See Figure 5b for the experimental setup.

is, exactly opposite the disturbance. This phenomenon, known as remote triggering, shows that the further away the positions are from the reference position the more pronounced is the antiphase behavior induced by the negative coupling, since at these positions the migration coupling, which opposes the negative coupling, is the smallest.

As we have seen, fronts in electrochemical systems show many different types of behavior depending on the experimental conditions and the arrangement of the electrodes. These behavior types are summarized in the simulations depicted in Figure 9. Standing domains form because of a close reference electrode and, thus, because of strong, negative global coupling as calculated by Christoph[35] (a). If the global coupling becomes weaker as the result of an increased distance of the reference electrode the transitions in the bistable regions are accompanied by fronts. The speed of these fronts decreases during the transition (b). For a remote reference electrode but close counter electrode (or equipotential plane), the migration coupling is local and, thus, the fronts move at a constant speed (c). If the distance between the working electrode and counter electrode is successively enlarged, the fronts are increasingly accelerated (d). Under galvanostatic conditions, namely, in the presence of a positive global coupling, the transition between both states takes place almost homogeneously (e).

3. Waves in Oscillatory Media

So far we have limited ourselves to phenomena that can be described by the spatiotemporal evolution of a single variable. Oscillating behavior and most wave phenomena arise because at least two variables interact. Simple periodic oscillations are often the result of so-called activator–inhibitor kinetics, especially in chemical reactions and in the electrochemical reactions presented here (Figure 10).[14] An activator is a variable that catalyzes its own production (thus it is autocatalytic), and that at the same time activates the formation of the inhibitor, that is, the formation of a second species (or variable). In contrast, the inhibitor impedes—or inhibits—the growth of the activator, and decays at a certain rate. The interaction between the activator and inhibitor represents a negative feedback mechanism: the activator induces its own decomposition through the formation of the inhibitor. Overall then, oscillatory behavior usually occurs together with autocatalysis and a negative feedback mechanism. The interaction of activator–inhibitor kinetic and transport processes or global coupling eventually results in chemical or electrochemical waves.

Electrochemical nonlinear phenomena can largely be placed into two classes of models:[37] The first class encom-

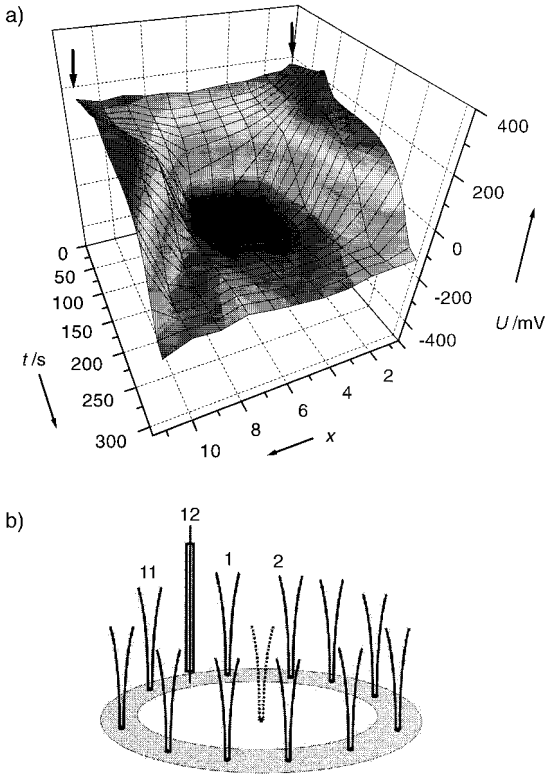

Figure 8. a) Local potential as a function of position and time during a remotely induced transition in the bistable regime of the oxidation of formic acid on a Pt ring electrode. The RE was positioned close to the WE. At the positions marked by the arrows the potential was disturbed locally toward positive values. The ring position gives the electrode number of (b). b) Setup for measurements used to obtain the data of (a). The outside potential probes serve to measure the local potential, the central one serves as the reference electrode. (This figure was provided by courtesy of P. Strasser and M. Eiswirth; see also ref. [36].)

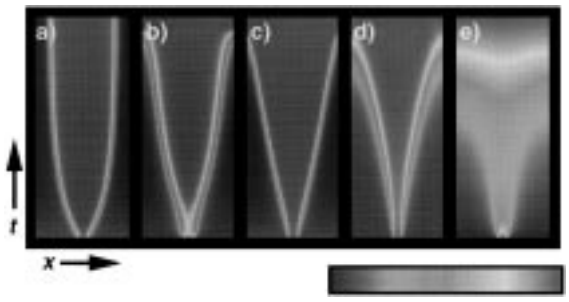

Figure 9. Simulation showing the influence of coupling on front behavior: a) for overcritical, negative global coupling, b) for less than critical, negative global coupling, c) without global coupling and a small distance between WE and CE (that is, approximate local migration coupling), d) without global coupling and a large distance between WE and CE (nonlocal migration coupling), e) under galvanostatic conditions, namely, with positive global coupling. The bar indicates the non-monotonic gray scale used.

passes systems that are connected to an N-shaped I/ϕ_{DL} curve and are known as N-NDR systems. As discussed above, such a relationship is linked to a self-enhancing change of ϕ_{DL} in certain ranges of the potential; ϕ_{DL} takes the role of the activator for N-NDR systems if two or more variables are necessary to describe the dynamic. Temporal and spatiotemporal dynamics of this type of oscillation are presented in this

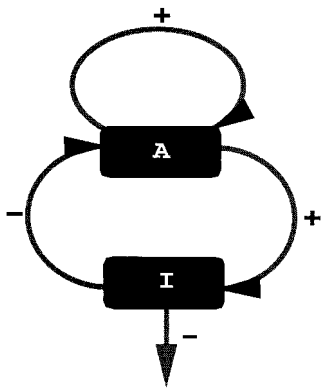

Figure 10. Positive (+) and negative (−) feedback between the activator (A) and inhibitor (I) variable.

section. The second class is connected to an S-shaped I/ϕ_{DL} curve, and ϕ_{DL} can be identified with the inhibitor.[38] The inhibitor is especially important for the formation of Turing-like stationary structures, and will be introduced in Section 4.1.

3.1. Homogeneous Dynamic

We can already find oscillations in N-NDR systems if the reaction current is determined to a large extent by the mass transport of the reacting species. The concentration of the reacting species takes the role of the inhibitor in N-NDR oscillations.[11] Figure 11 shows how the feedback of a slow

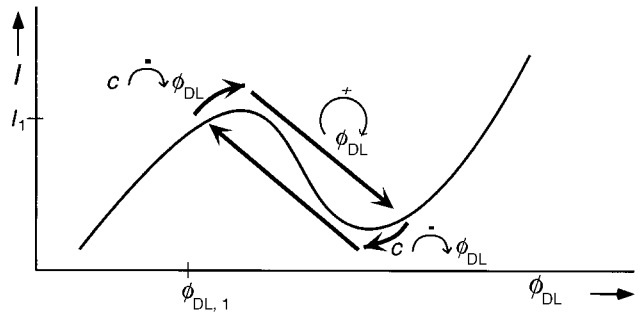

Figure 11. Illustration of how oscillations occur in N-NDR systems as a result of the interaction of electrode potential and concentration in the case of the slow transport of the reacting species.

mass transport onto ϕ_{DL} can lead to oscillations. The depicted N-shaped I/ϕ_{DL} curve represents a "base" relationship, in which base means that the concentration of the electroactive species has the same value in the reaction plane for all potentials. This situation corresponds to the limiting case of infinitely fast transport. For slower transport, however, the concentration of the reactant in front of the electrode will be reduced the most at potentials for which the current is the largest. Let us assume that at the start of an experiment, that is, at a time when the concentration in front of the electrode equals that of the bulk, a state would be taken on the first branch of the I/ϕ_{DL} curve relatively close to the current maximum (for example, $I_1/\phi_{DL,1}$ in Figure 11). The consump-

tion of the reactant would initially be larger than the replenishment by the transport; the concentration and, thus, the current would therefore decrease slowly. However, the potential drop in the electrolyte is smaller for a lower current density, which results in an increase of ϕ_{DL} under potentiostatic conditions. Therefore, ϕ_{DL} is pushed to higher values because of the slow transport. If ϕ_{DL} reaches the range of negative differential resistance ϕ_{DL} is "produced" autocatalytically according to the same mechanism discussed in Section 2.1 for bistable behavior. This "production" continues until ϕ_{DL} takes values on the outer branch of the N curve. The current is much less for these values than for our starting potential, and the concentration of the electroactive species increases again at this low reaction rate. Accordingly, the current then increases slowly, and thus, the potential moves to lower values until autocatalysis starts up again. In this way, the system reaches a situation similar to that of the starting situation, and the cycle starts anew.

Oscillations in all oscillating systems occur only in certain ranges of the external parameters. For example, the conductivity of N-NDR systems cannot be too large or too small. It should be mentioned, however, that the only demand on the electrode kinetic is still the occurrence of a negative differential resistance. This is part of the reason why oscillations appear much more often in electrochemistry than, for example, in chemical reactions in a homogeneous phase. However, potential-dependent processes that take place at the interface often also result in a negative feedback.[7, 8, 39, 40] These latter electrochemical systems have a different phase or bifurcation diagram in the parameter plane spanned by the external voltage and the electrolyte resistance than the systems discussed above.[7, 8] The biggest difference is that these systems oscillate under galvanostatic conditions, which is in contrast to the oscillator-type we looked at above. A current–voltage relationship with a negative impedance is also a necessary prerequisite for this type of oscillator. However, in the stationary current–voltage curve, this negative impedance is visible only in a subsystem. Other electrode processes take place in the total system in parallel to the reaction steps of the subsystem and cover the typical N-shape or at least a region of the negative differential resistance. If the steps hiding the negative differential resistance are slow compared to typical changes of ϕ_{DL}, the stationary I/U relationship becomes unstable under galvanostatic conditions and for high values of electrolyte resistance (or, generally, for a sufficiently large resistance in series to the working electrode). Furthermore, oscillations occur. Since the negative differential resistance does not surface in the range of the oscillations for the total system, the connotation for this N-NDR subsystem has an additional "H" (for hidden) to differentiate it from the systems described above.[8, 39]

Typical representatives of HN-NDR oscillators are oxidation reactions of small organic molecules such as formic acid,[41, 42] formaldehyde,[43] or methanol.[44] Furthermore, the electrochemical dissolution of nickel[7, 45, 46] or the oxidation of hydrogen in the presence of certain cations and anions[8] can be attributed to this oscillator type.

As we have seen, bistable behavior in N-NDR systems turns into oscillatory behavior only because the rate of the electrode reaction becomes transport-limiting. In the case of an HN-NDR oscillator, a rate-limiting transport represents a negative feedback as well. Therefore, HN-NDR systems with a mass transport limiting reaction rate often require the consideration of a third variable, the concentration of the reacting species in front of the electrode. Hence, such HN-NDR systems possess two feedback loops. Dynamic systems such as these, that is, systems with three variables: autocatalysis and two negative feedback loops, can also exhibit more complex temporal behavior.[16]

The best known and most spectacular of these behaviors is certainly deterministic chaos. There are numerous electrochemical examples of deterministic chaotic oscillations in the potential or the current. Aside from chaotic behavior, many studies involved mixed-mode oscillations (MMOs). These are characterized by an alternating sequence of a certain number of oscillations with small and large amplitudes. A characteristic pattern of small and large amplitudes usually exists only in a small parameter interval. If an experimentally controllable quantity is changed complicated sequences are observed (Figure 12), whose underlying mathematical structure could be uncovered by a number of theoretical studies.[47, 48]

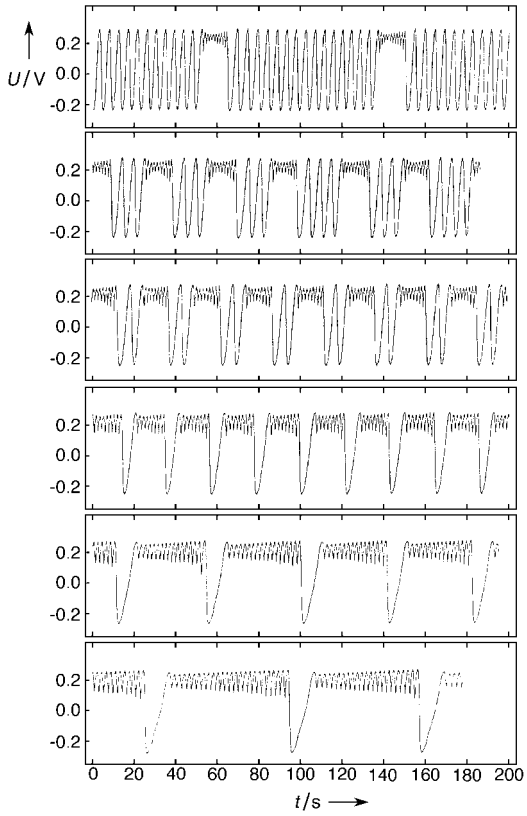

Figure 12. Mixed-mode oscillations during galvanostatic oxidation of H_2 on a Pt electrode in the presence of Bi^{3+} and Cl^- ions. The transition between the forms of oscillation was caused by a minor change in the set current.

The chemical and electrochemical processes leading to negative differential resistance or to negative feedback for HN-NDR oscillators can be discerned for a number of reactions. However, the physicochemical origin of the second feedback loop, and thus, the occurrence of chaos or MMOs

has been identified in only a few examples. It is easy to conclude that slower transport for HN-NDR systems can result in more complex temporal behavior. However, up to now, studies indicate that slower transport is not responsible for the occurrence of MMOs or chaotic oscillations under galvanostatic conditions.[8, 42] Nonetheless, MMOs or chaotic oscillations occur with almost all HN-NDR oscillators.

In contrast, the origin of mixed-mode oscillations in the first described N-NDR oscillators appears solved and seems to be independent of electrode processes. Koper and Gaspard showed that slow transport can provide not just one but two degrees of freedom.[49] This result can be explained by a concentration change in an expanded range in front of the electrode. The whole concentration profile perpendicular to the electrode does not adjust spontaneously to a concentration change at the electrode caused by a high reaction rate. Rather, the adjustment of concentration at larger distances shows a delay, which manifests itself as a new degree of freedom in the dynamic. Although most of the observed complex oscillations are a result of other feedback loops, we have to point out how small the demands on the electrochemical processes are in order to be sufficient enough to cause an enormous variety of dynamic features for electrochemical reactions.

3.2. Primary Spatial Instability of the Simple Limit Cycle

Altogether, the number of studies on spatial pattern formation for oscillating electrochemical reactions is relatively small—probably because of experimental difficulties. Some studies, however, provide evidence that electrochemical oscillations can be accompanied by waves. In 1844, Joule[50] already pointed out that the periodic formation of a "white layer" observed during the dissolution of iron is not homogeneous. On the contrary, a film starts to propagate across the surface of the electrode during a certain phase of the current oscillation. Since this report, the "iron oscillator" has been renowned for exhibiting a variety of sometimes spectacular waves, such as a spatiotemporal period doubling.[51, 52] These observations appear to be just the tip of the iceberg. The periodic variation in the current is accompanied by the formation of sometimes surprisingly complicated waves in other oscillating electrode reactions. Examples of these reactions are the electrodissolution of nickel or cobalt, the oxidation of formic acid or hydrogen, and the reduction of peroxodisulfate.[53]

Analysis of the patterns as well as of the conditions under which spatial pattern formation takes place is normally complicated in electrochemical systems because different reaction conditions exist on the electrode boundaries compared to those at the center of the electrode. The different reaction conditions could be a consequence of a difference in concentrations or in "effective conductivity". Thus, the parameters vary along the radial coordinate of a disk electrode.[8, 35] The situation is different for ring electrodes: If the width of the ring is much smaller than its diameter, pattern formation takes place only along the angular coordinate. However, most observed patterns are also not understood for such ring electrodes. Therefore, we concentrate on a few examples of pattern formation on ring electrodes. In this section we discuss phenomena that arise because of the interaction of migration coupling and the dynamic of the homogeneous system.[54] In Section 3.2 we discuss phenomena that require the presence of a negative global coupling.

Let us first look at simulations that are based on N-NDR oscillators with two variables (see Appendix and Figure 13). These simulations show that the homogeneous oscillation can become unstable starting at a certain length of the electrode (Figure 13 a).[55] The two figures in the top row document how the system becomes unstable with respect to minute spatial inhomogeneous disturbances after a minor elongation of the

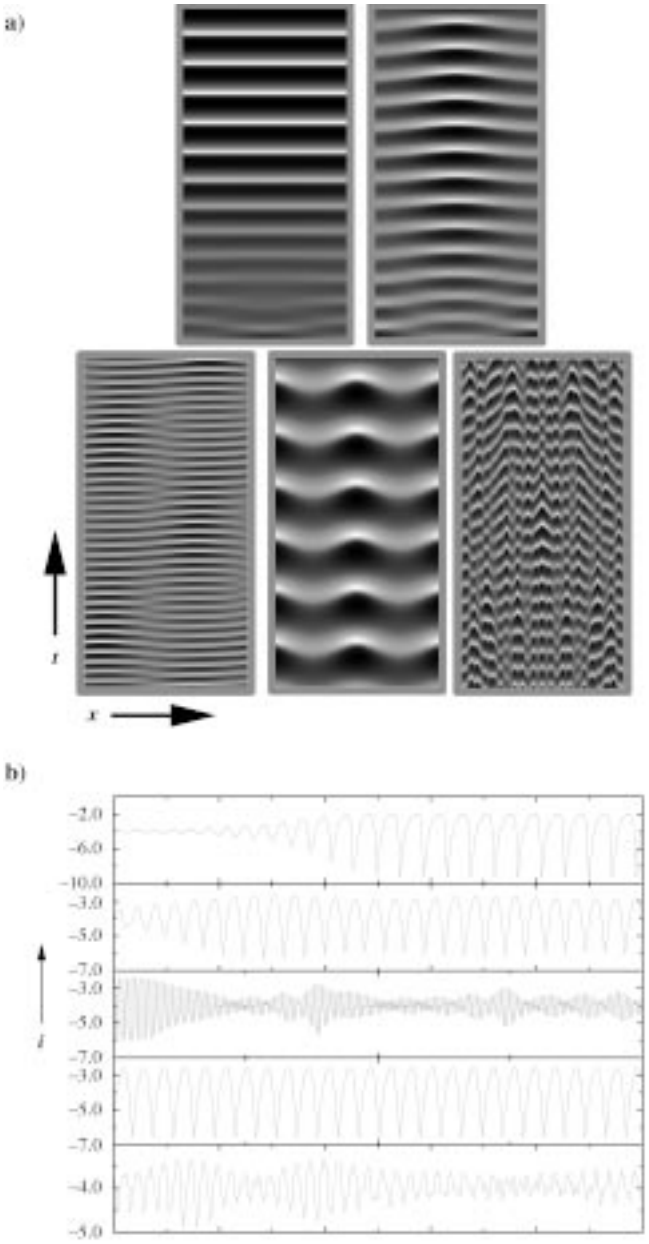

Figure 13. Simulation of a) the spatiotemporal evolution of the double-layer potential and b) the corresponding total current of an N-NDR oscillator for an electrode length that increases from left to right and top to bottom.

electrode, which results in formation of a wave. In both cases a small sine-shaped perturbation was added to the homogeneous oscillation at a certain time. Clearly, the disturbance is dampened in the first picture, whereas a spatiotemporal structure forms in the second example. This structure can best be described as a superposition of the homogeneous oscillation and a sine-shaped standing wave. A further increase in the length of the system leads to a complicated sequence of aperiodic and periodic waves; three examples are seen in the bottom row of Figure 13a.

Figure 13b shows the total current that corresponds to the spatiotemporal plots of Figure 13a. Two things should be pointed out here: First, the primary instability of the homogeneous oscillation cannot be discerned from the global time series; in the first two situations the time series are simple-periodic after a transient time, which depends on the chosen starting conditions. Second, the time series of the total current corresponding to the aperiodic spatial evolution of the double-layer potential are not simple-periodic. Thus, the dynamic can very well get complex in the model with two variables if spatial instabilities participate. Above we stated that one needs the interaction of at least three variables for more complex behavior; this is true only for the homogeneous case. The spatial coordinate provides the system with additional degrees of freedom, which make it possible to have a not completely synchronous evolution of the individual positions.

The critical electrode length at which wave phenomena develop at the electrode depends on the parameters of the system, especially the rate constants as well as the conductivity of the electrolyte. We should stress that so far the observed wavelengths were in the range of mm to cm, that is, in macroscopic and not in mesoscopic or microscopic dimensions. Exceptions to this are two systems, the dissolution of Ag-Sb alloys[56, 57] and the oxidation of Al in the electropolishing regime.[58]

The transition from homogeneous oscillations to spatiotemporal chaotic behavior shown in Figure 13a is characteristic for spatially expanded (unstirred) oscillating systems. Nevertheless, to the best of our knowledge, no experiments have so far proven the primary instability of a homogeneous oscillation among chemical oscillators. Recently, we achieved the first evidence in an electrochemical system, the galvanostatic oxidation of H_2 in the presence of Cu^{2+} and Cl^- ions on a Pt ring electrode.[59] As for previous experiments, the setup for this experiment was analogous to the one depicted in Figure 5b. The spatiotemporal evolution of the double-layer potential can be seen in Figure 14a. For the sake of clarity the homogeneous oscillation was subtracted in this figure so that the resulting dynamic displayed shows the spatially inhomogeneous part of the potential distribution only. It is clear from Figure 14b that the oscillations have a strong relaxationlike character. The inhomogeneous structure forms mainly at the two flanks of the oscillation. The total dynamic can be viewed as a superposition of a homogeneous oscillation and a standing wave, similar to the second simulation displayed in Figure 13a.

Another impressive example was measured by Otterstedt et al. for cobalt dissolution.[60] This example stresses the variety of phenomena that have yet to be investigated and

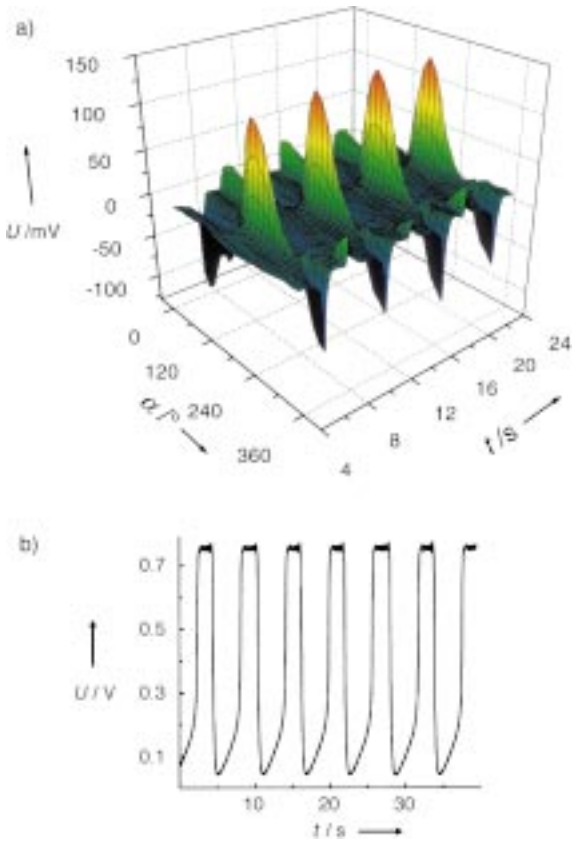

Figure 14. a) Spatiotemporal evolution of the potential at a Pt electrode during the oxidation of H_2 in the presence of Cu^{2+} and Cl^- ions after subtraction of the homogeneous oscillating part. b) Temporal evolution of the total current. The first four oscillations correspond to the time interval shown in (a). See Figure 5b for the experimental setup.

understood. The experiment was performed under potentiostatic conditions with a narrow cobalt strip, that is, with essentially one-dimensional electrodes. The dissolution of cobalt is oscillatory for certain values of the externally applied voltage. Current oscillations are always relaxationlike and, as long as the current oscillations are simple-periodic, active zones form at both rims of the strip. These zones expand in an accelerated fashion toward the center. This behavior appears similar to that found for accelerated transitions in the bistable regime and can probably also be explained with nonlocal migration coupling. If the parameters are varied, the activation phase becomes longer and is superposed by small oscillations (Figure 15a). These small oscillations arise from oscillations in the width of the active range: The motion of the leading front is an accelerated motion (Figure 15b); the back front displays a pulsating behavior in the passive range, however. Similar phenomena are also observed for the dissolution of cobalt in the excitable range of the reaction.[61]

3.3. Standing Waves and Pulses through Negative Global Coupling

The spatiotemporal behavior changes qualitatively in the oscillating range if the reference electrode is close to the working electrode, that is, if a negative global coupling is

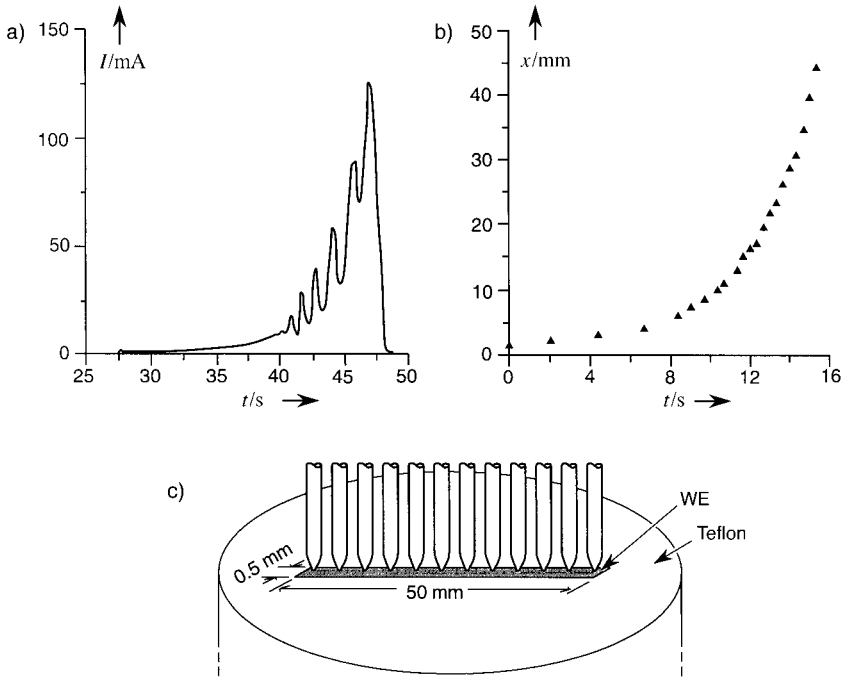

Figure 15. a) Total current and b) position of the leading front as a function of time for a single autonomous oscillation during dissolution of cobalt. c) Electrode geometry and arrangement of the potential probes to measure the spatiotemporal evolution of the potential. (Reproduced with permission from ref. [60].)

present.[35, 62] As is immediately clear from the possibility of triggering fronts remotely (see Figure 8), regions far away from each other behave anticorrelated if a negative global coupling acts on the autocatalytic variable (in our case the double-layer potential). A homogeneous oscillation in which all positions of the electrode oscillate in phase becomes unstable at a critical strength of the negative coupling. The system then makes way for an inhomogeneously oscillating state. As a typical behavior, standing waves then occur with wave number 1 as do so-called phase pulses.

It is intuitively understood that standing waves arise because of a negative global coupling: Two domains form as a consequence of the antiphase behavior of regions remote from each other. These domains oscillate 180° out of phase. If the values of the parameters are close to those needed for the onset of oscillations, the distribution of the amplitude forms a sine structure in space. The wavelength of this sine curve is equal to the length of the system. The standing oscillation can be approximated by a sine profile oscillating in time. The sine wave possesses two nodes, that is, two positions hat are stationary in time.[63] This is a vital difference to the wave phenomena described in Section 3.2, in which the homogeneous mode is always oscillating as well. Standing waves have been observed experimentally for the oxidation of formic acid at Pt ring electrodes (Figure 16), whereby the experimental setup was analogous to that shown in Figure 8.[64]

If besides a sine profile, the 90°-rotated structure, the cosine profile, also oscillates in time the standing wave is transformed into a phase pulse or a travelling wave. The symmetry of the system implies that the stability behavior of ring electrodes is the same with regard to sine-shaped and cosine-shaped excitations. If both modes are excited because of an asymmetrical perturbation, a phase pulse forms.

Pulses were already measured by Otterstedt et al. in pioneering experiments with a close reference electrode.[65] These again were experiments on the electrodissolution of cobalt. The experiments were performed with ring as well as with disc electrodes. The experimental setup was chosen such that the surface of the working electrode was facing up. Since passive and active ranges of the electrode have a visible contrast, the spatiotemporal dynamic could be followed with a video camera (Figure 17 A). The pulses could be seen as narrow, travelling domains of high activity, that is, a high rate of dissolution, on an otherwise passive electrode. An example of a cobalt pulse rotating around the center of a disc electrode is depicted in Figure 17 B.

Besides standing oscillations and pulses, the theoretical studies cited above predict a variety of different patterns in oscillating media with negative global coupling. Most

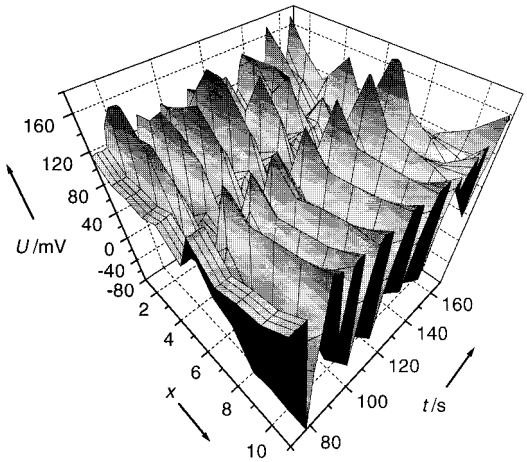

Figure 16. Standing wave for a close RE during potentiostatic oxidation of formic acid on a Pt ring electrode. See Figure 8b for the experimental setup. (This figure was generously provided by P. Strasser and M. Eiswirth, see also ref. [64].)

of them, however, exist only in substantially smaller ranges of the parameters and so far could not be proven experimentally. An exception appears to be so-called one-dimensional target patterns.[32] For these patterns, two pulses are sent at periodic intervals from one place of the ring electrode. The pulses travel in opposite directions and cancel each other when they meet at the opposite side. A similar behavior was found likewise for the electrodissolution of cobalt, although the pulse shows aperiodic modulations in the width. The authors suspect that this is the result of the chemistry of cobalt dissolution being more complicated, and cannot be described with two variables only, unlike the assumption made for all other simulations.

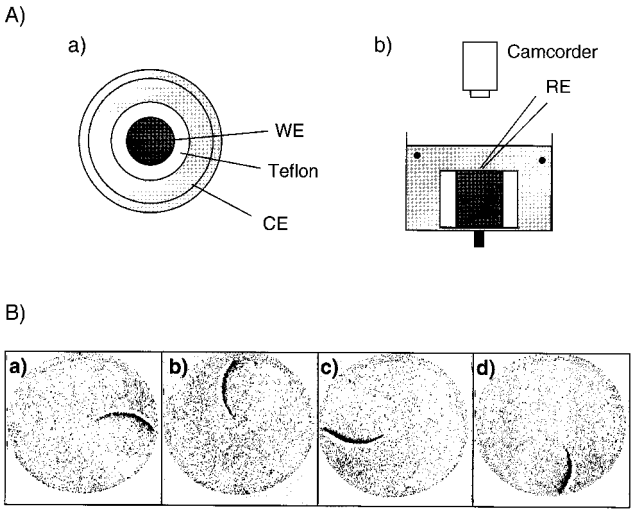

Figure 17. A) a) Top view and b) side view of experimental setup. B) Rotating active region during the oxidation of a disc-shaped Co electrode with a close RE. (This figure was generously provided by R. D. Otterstedt et al., see also ref. [60].)

4. Stationary Structures

So far we have only looked at electrode reactions that are connected to an N-shaped I/ϕ_{DL} curve, with ϕ_{DL} being the autocatalytic variable. Another type of I/ϕ_{DL} curve exists that has a negative differential resistance, but shows an opposing behavior with respect to pattern formation. These curves have the shape of an "S", and the double-layer potential represents the feedback variable, the inhibitor. In this case, the migration coupling does not result in motion of potential fronts, but favors formation of stationary potential patterns. These patterns have a defined wavelength for sufficiently large electrodes.[38] The wavelength is determined solely by the rate constant and by other system parameters, but not the length of the system as is the case for the stationary potential domains described in Section 2.3.

4.1. Homogeneous Dynamic

An S-shaped current–potential curve only exists if the dynamic of a chemical variable, that is, of a concentration or coverage of the electrode, is connected to an autocatalytic process that is potential-dependent. This could be a chemical, autocatalytic reaction step as was discovered for zinc dissolution, for example.[66, 67] In addition, a self-enhancing feedback is also caused when attractive interactions between adsorbed molecules are strong enough. In this case, the adsorbing species exist in two phases depending on external parameters. The phases can be, for example, a well-ordered monolayer and a two-dimensional gas, that is, a state in which the adsorbed molecules move in an uncorrelated manner on the surface of the electrode. A transition between both phases can be induced by variations of ϕ_{DL}, for example, and takes place as a first-order phase transition.[68] Hence, there is a certain range of potential in which both phases can coexist, one as a metastable phase and the other as a globally stable one. These types of overcritical, attracting interactions have been found for a variety of adsorbates.[69] If the two phases inhibit an electrode reaction differently, the corresponding current–potential relationships display an S- or Z-shaped I/ϕ_{DL} curve.

The central branch of the S-shaped curve clearly has a negative differential resistance (Figure 18a); this, together with the external potentiostatic or galvanostatic control, leads to a negative feedback loop that can stabilize a state on the

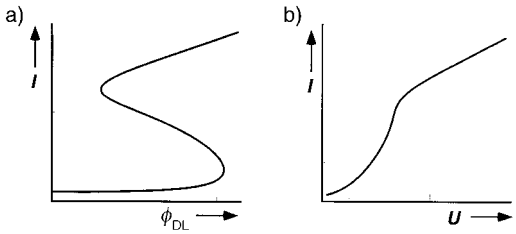

Figure 18. a) Schematic representation of an S-shaped current–electrode potential relationship. The branch with low current corresponds to high values of the potential and vice versa. b) Monotonic current–voltage curve.

NDR branch. This stabilization occurs for overcritical electrolyte resistance and manifests itself in a unique current–voltage curve (Figure 18b). The following helps to explain this: Let us assume that the system is at a state on the central potentially unstable branch of the I/ϕ_{DL} curve. Let us assume further that the system succumbs to a fluctuation toward more positive values of ϕ_{DL}. The system reacts to this perturbation foremost by autocatalytically desorbing the adsorbate (that is, we arrive at the top current branch of Figure 18a). The potentiostatic control, however, causes the increase of the current to produce smaller values of ϕ_{DL}. Thus, the fluctuation of ϕ_{DL} is suppressed.

This consideration allows us to easily see that the feedback in the potential gets so big at a critical value of the electrolyte resistance that the system periodically oscillates between the two outer branches of the I/ϕ_{DL} curve when fast changes in the coverage occur. Normally however, the characteristic time during which the potential changes is short in comparison with that of chemical concentrations or adsorbate coverage. Oscillations for systems with S-shaped current–potential curves are therefore more the exception than the rule. Rather, the system assumes a stationary state on the negative differential branch. However, this state is probably spatially structured. As will be explained in the next section in more detail, the migration coupling destabilizes the homogeneous state. For a sufficiently large electrode, these stationary, nonequilibrium patterns appear in S-NDR systems as easily as oscillations in N-NDR systems.

4.2. Turing Patterns in Electrochemical Systems

The mechanism of formation and the properties of stationary patterns of the potential are analogous to those of the famous Turing patterns.[70] These patterns, predicted by Turing in 1952, are stationary concentration patterns that can form

spontaneously in activator–inhibitor systems if the inhibitor diffuses faster than the activator.

Figure 19 shows how the interaction of reaction and diffusion leads to formation of stationary patterns. The starting point is a homogeneous state that is slightly disturbed

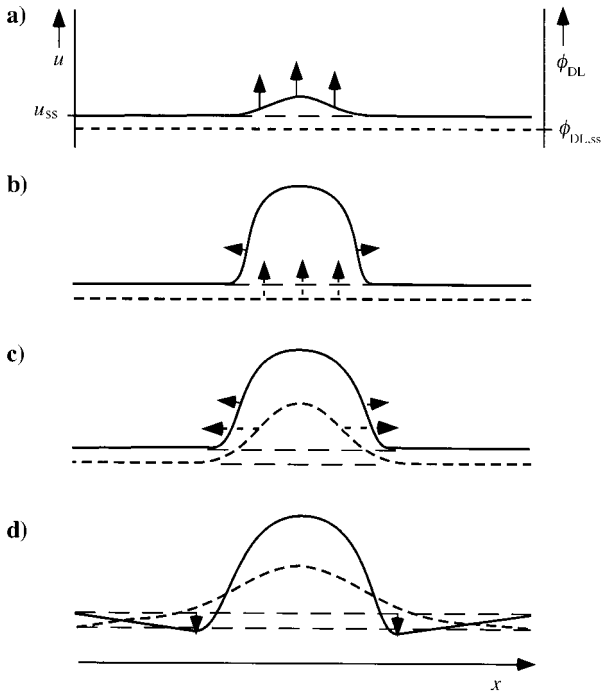

Figure 19. Evolution of a stationary structure in activator–inhibitor systems with fast transport of the inhibitor. ("ss" as well as curves with long dashes denote the value of the activator or inhibitor at the homogeneous fixed point; curve with solid line: activator profile; curve with short dashes: inhibitor profile.)

by a small local fluctuation in the concentration of the activator (solid line; a). The fluctuation is enhanced as a result of the autocatalytic nature of the activator kinetic (b). An increased activator concentration causes the inhibitor to be produced (short dashed line; c). In the S-NDR systems, for example, an increase in the coverage causes the potential to be moved to larger values, which is equivalent to the production of inhibitor. Thus, the local perturbation produces a region with higher activator and inhibitor concentration. In turn, a flux of activator and inhibitor in the neighboring region is induced. Since the inhibitor diffuses faster than the activator, the inhibitor also builds up faster than the activator in a certain neighboring region around the local spot (d). A high value of the inhibitor variable leads to a decay of the activator concentration. In our electrochemical system, for example, a high electrode potential brings about the desorption of the adsorbate.

Hence, a small local perturbation of the homogeneous state leads to a larger region of increased activator concentration because of the interaction of reaction and diffusion. Inhibitor is always produced in this region and is transported to neighboring domains. Since the inhibitor concentration is increased in the neighborhood of the local spot, the activator concentration is kept very small outside of it. In this way, a stable stationary structure arises. An outstanding property of Turing patterns is that they are periodic patterns with a characteristic wavelength that depends solely on the reaction constants and the diffusion constants.

As we have seen, diffusion, a transport process that by itself balances any inhomogeneities over time, can destabilize a homogeneous state when interacting with certain nonlinear kinetics and can lead to the formation of concentration gradients. This fascinating fact prompted an intense search for experimental examples. However, the search for stationary Turing patterns was not successful until 40 years after Turing's theoretical prediction.[71] The reason for this is that it is difficult to find systems in which the diffusion coefficient of the inhibitor is sufficiently greater than that of the activator. This limitation does not exist in electrochemical systems: Here the electrode potential acts as the inhibitor, and the corresponding transport process is migration. The characteristic time of migration is always shorter than the characteristic time of diffusion[72] of the autocatalytic species. Thus, stationary potential patterns in S-NDR systems occur almost always when the total current is in the range of the central branch of the current–potential curve (provided that the electrode is at least as big as the wavelength of the Turing structure). This has been discovered in theoretical studies only recently[38] and were proven experimentally shortly after.[73] A simulation of electrochemical Turing structures is shown in Figure 20. Here we stress again that these structures have a characteristic wavelength in contrast to all patterns that arise from global coupling.

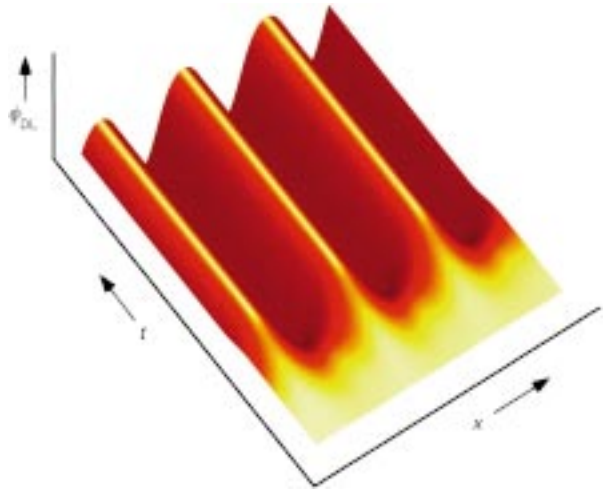

Figure 20. Simulation of spatiotemporal behavior in S-NDR systems showing the outgrowth of a stationary structure from the homogeneous state.

5. Summary and Outlook

A breakthrough was achieved in the understanding of pattern formation in electrochemical systems in the past decade. Two results caused this progress: the understanding that temporal instabilities, or, to put it more broadly, instabilities of the homogeneous system, arise in most cases because of a negative differential resistance in the I/ϕ_{DL} characteristic, and the understanding that a local change of

the potential distribution of the double layer changes the migration currents on the total electrode/electrolyte interface. Therefore, this migration coupling largely determines the formation of spatial patterns. In both cases, the electrical properties of the electrochemical systems are very important, and the electrode potential is an essential variable (that is, a variable necessary for the description of self-organization phenomena). The corresponding evolution law is obtained from the local charge balance at the electrode, and constitutes a reaction – migration equation.

Electrical properties determine the particularities of pattern formation in electrochemical systems. In contrast, the pattern formation of chemical systems in a homogeneous phase is described by reaction – diffusion systems. First let us compare the two transport processes, migration and diffusion: The conductivity of the electrolyte determines how fast inhomogeneities of the potential are adjusted by migration. The conductivity is a quantity that can be varied experimentally over several orders of magnitude. The rate of diffusion, however, is determined by the diffusion constant, whose experimental variation is very limited; it is mainly restricted to temperature changes. However, the ratio of the characteristic times of the homogeneous dynamic, that is, of the reaction term, and of the transport processes crucially influences the patterns. This influence can be investigated easily for electrochemical systems, and can be exploited to a certain degree to adjust specific patterns or to avoid spatial inhomogeneities.

The range of the coupling is a further important difference between the diffusive coupling and the coupling by migration. Diffusive coupling is a nearest-neighbor coupling; in this sense, it is local. Migration coupling, however, is nonlocal, that is, a change of state at a particular location induces noticeably and instantly changed migration currents at the electrode in an expanded, surrounding area. Nonlocal coupling thus leads to the occurrence of accelerated fronts. The extent of nonlocal coupling depends on the geometry of the cell, namely, on the distance between the working electrode and counter electrode (or an equipotential plane parallel to the electrode). The smaller this distance, the smaller the range of the coupling. In the extreme case of an infinitely small distance, nonlocal coupling turns into diffusive coupling. Thus, electrochemical systems possess the peculiarity that the range of the spatial coupling can be varied as can the characteristic time of the spatial coupling.

Two kinds of global coupling can occur aside from the migration coupling, depending on experimental conditions. If the distance between the working electrode and the reference electrode is small the feedback over the potentiostat results in a negative global coupling. This negative global coupling induces an antiphase behavior. In contrast, a positive global coupling exists for galvanostatic conditions which acts by synchronizing itself.

All three types of coupling, migration coupling, as well as negative and positive global coupling depend solely on the electrical properties of the system. Therefore, they are independent of the electrode reaction. Thus, everything we summarized up to now applies to all electrochemical systems. The type of pattern for a given system depends on the interaction of spatial coupling and the dynamic of the homogeneous system. Here, the electrode reactions come into play. According to the present state of research, electrode reactions can be divided into just two classes under conditions for which instabilities are observed despite large chemical variations: systems with N-shaped I/ϕ_{DL} curves, and systems with S-shaped I/ϕ_{DL} curves. Both classes are activator – inhibitor systems as are chemical reactions that oscillate in homogeneous phase. The electrode potential is the activator for N-NDR systems and the inhibitor for S-NDR systems. Thus, the three types of spatial coupling discussed above act either on the activator variable or on the inhibitor variable. The variety of combinations results in a broad spectrum of spatial instabilities and patterns. These are summarized in Table 1.

If the electrode potential represents the activator, the migration coupling leads to fronts and waves, which often propagate in an accelerated manner because the coupling is nonlocal. An additional positive global coupling enhances the accelerated expansion on the one hand, and, on the other hand, can result in the formation of domains in the oscillatory range.[74] However, if a negative coupling superposes the migration coupling then standing domains, standing waves with wave number 1, or pulses can form, depending on the parameters. If the electrode potential is the inhibitor, the migration currents can destabilize a homogeneous potential distribution in a Turing-like instability, and stationary patterns with a characteristic wavelength result. Since migration currents and positive global coupling act similarly in S-NDR systems, positive global coupling leads to the formation of stationary domains as well. The wavelength of the domains, however, is then the same as the length of the system. Negative global coupling, on the other hand, changes pattern formation only qualitatively if the system oscillates. In this case, negative global coupling can result in the formation of standing waves with wave number 1 just like in N-NDR

Table 1. Typical phenomena of pattern formation in N-NDR and S-NDR systems with different types of spatial coupling.[a]

	Nonlocal migration coupling (always present)	Negative global coupling:potentiostatic control with Haber – Luggin capillary	Postive global coupling:galvanostatic control
N-NDR systems: ϕ_{DL} = activator	accelerated waves	stationary domains, standing waves ($n=1$), phase pulses	enhanced acceleration of potential fronts, mainly homogenizing effect; cluster formation in the oscillatory region
S-NDR systems: ϕ_{DL} = inhibitor	Turing-like structures with intrinsic wavelength ($n \geq 1$)	standing waves ($n=1$), or mixed-mode patterns with $n_1 > 1$, $n_2 = 1$; phase pulses	stationary domains ($n=1$ or $n>1$)

[a] n is the wavenumber of the resulting pattern.

systems. For parameter values for which the migration coupling leads to the formation of Turing-like structures, the interaction of both instabilities can yield a complex wave pattern characterized by the two wave numbers $n=1$ and $n>1$.[75] However, oscillations normally do not occur in S-NDR systems. Therefore, the latter patterns are expected to be observable only in exceptional cases.

It may appear that Table 1 contains an essentially complete summary of patterns that occur in electrochemical systems. This appearance is misleading. Table 1 only roughly summarizes results observed so far or predicted with models. These are investigations concentrating on phenomena that can be described with two essential variables (two-component systems). Furthermore, the phenomena are restricted to the basic patterns that are common and exist in a large parameter range. Additional experiments, especially in the oscillatory range, will certainly call for supplementation in the individual cells.

Moreover, the number of rows and columns of the cell will have to be increased: Numerous examples of current or potential oscillations involve complex time series. Only in a few cases does the complex time series result from the spatial patterns. Initial simulations of such behavior are depicted in Figure 13, and the first spatiotemporal structure of this series has recently been demonstrated (Figure 14). In most cases the additional degree of freedom will be from a third dependent variable such as from a concentration that adds an additional feedback loop into the system as discussed in Section 3.1. Spatial pattern formation in three-variable systems is an area that is currently developing strongly, not just in electrochemistry but generally in nonlinear dynamics. Aside from increasing the number of rows, the number of columns should also be increased. So far, it has always been assumed that concentration differences in the electrolyte can be neglected in theoretical studies as well as in the interpretation of the observed patterns. This assumption may no longer be justified for high current densities. Electrohydrodynamic convection develops from a critical current density on, and this is an additional transport mechanism that by itself leads to pattern formation and can also interact with the already discussed modes of spatial coupling.

This listing is still not complete. However, it shows some central questions and future directions in the study of self-organization phenomena in electrochemical systems. An additional, important development of research activities in the area of the nonlinear dynamic in electrochemistry is applied research. A big challenge in the next few years will be to use the knowledge obtained so far on instabilities to improve industrial processes. Here, an important and promising aspect would be to increase the yield by carrying out a reaction under conditions for which the reaction proceeds in a nonstationary or inhomogeneous manner. To apply this already old idea to electrochemical systems seems especially promising since a number of electrical parameters are available in these systems. These parameters crucially determine the dynamic and can easily be controlled experimentally. Initial experimental indications have been presented recently that suggest that nonstationary experimental conditions may actually be superior to stationary ones.[76]

An important aspect of investigations of pattern formation in chemical systems has always been that these systems can function as models, especially for biological systems. The contribution of the investigations is, without doubt, highly significant for the understanding of biochemical oscillations, cellular rhythms, or even the formation of spatial patterns as, for example, during the developmental phase of the slime mold *Dictyostelium discoideum*. Early studies on pattern formation in electrochemical systems were motivated by the similarity of potential waves that had been observed for metal dissolution reactions and the propagation of electrical signals in the nervous system. Up to now, a central role has been assigned to the universal aspect of research of nonlinear phenomena, which establishes the continued interdisciplinary interest on chemical nonequilibrium structures. Electrochemical systems are ideal model systems for a variety of processes of pattern formation, particularly if they involve the interaction of chemical and electrical properties. Such systems are often encountered in biological systems, such as, for example, in biophysical membrane oscillations.

Appendix

In this appendix we list the minimal equations (prototype equations) that describe the phenomena of self-organization discussed in the individual chapters. Figures 9, 13, and 20 are based on these equations. All symbols used are explained at the end of the Appendix.

Section 2: The phenomena discussed in Section 2 are described by the spatiotemporal evolution of only one degree of freedom (a single variable). All examples shown here apply to N-shaped current–voltage curves, for which ϕ_{DL} is the essential variable.

The dynamic of the homogeneous system is given by Equation (1),[7, 8] where $k(\phi_{DL})$ has an N-shaped dependence

$$C\frac{d\phi_{DL}}{dt} = -nFc_b k(\phi_{DL}) + \frac{U-\phi_{DL}}{RA} \quad (1)$$

on ϕ_{DL}. In most cases, this dependence is described as a polynomial of third degree. The first term on the right side of the equation describes the reaction current density, the second term describes the total current normalized to a unit area. For the spatially expanded system, the last term of Equation (1) has to be substituted with the local migration current density that exists in front of the electrode [Eq. (2)],[8] where the potential in the electrolyte is obtained by solving Laplace's Equation (3). The boundary conditions follow from the cell geometry.

$$C\frac{\partial\phi_{DL}}{\partial t} = -nFc_b k(\phi_{DL}) - \sigma\left.\frac{\partial\phi}{\partial z}\right|_{z=WE} \quad (2)$$

$$\Delta\phi = 0 \quad (3)$$

For the simulations depicted in Figures 9, 13, and 20, the ring-shaped working electrode was approximated by an infinitesimally thin ring, and the electrolyte by a cylindrical surface, which was confined by the working electrode on the one side and the counter electrode on the other side

[Eqs. (4)–(6)]. ϕ_{DL} and ϕ are connected by the potentiostatic [Eq. (7)] or the galvanostatic [Eq. (8)] control conditions.

$$\phi(x+L,z,t)=\phi(x,z,t) \tag{4}$$

$$\phi(x,z=\mathrm{CE},t)=0 \tag{5}$$

$$\phi(x,z=\mathrm{WE},t=0)=\phi^0 \tag{6}$$

$$U=\phi_{DL}+(\phi\mid_{z=\mathrm{WE}}-\phi\mid_{z=\mathrm{RE}}) \tag{7}$$

$$I_{tot}=-\sigma\int_0^L \left.\frac{\partial\phi}{\partial z}\right|_{z=\mathrm{WE}} \mathrm{d}x \tag{8}$$

The potentiostatic control condition adds a negative global coupling into the system if the reference electrode is not at the level of the counter electrode. In this case, as well as in the galvanostatic case, for which the global coupling is positive[34] Equation (2) can be rearranged such that it contains a term that is proportional to the mean of ϕ_{DL}.[31] The proportionality factor is negative for negative global coupling and positive for positive global coupling.

Section 3: The homogeneous dynamic of the standard model for N-NDR oscillators is given by the coupled Equations (9) and (10).[7, 8] The changes of concentration arise from

$$C\frac{\mathrm{d}\phi_{DL}}{\mathrm{d}t}=-nFck(\phi_{DL})+\frac{U-\phi_{DL}}{RA} \tag{9}$$

$$\frac{\mathrm{d}c}{\mathrm{d}t}=-\frac{2}{\delta}ck(\phi_{DL})+\frac{2D}{\delta^2}(c_b-c) \tag{10}$$

reaction and diffusion perpendicular to the electrode [first and second term on the right side of Eq. (10)]. In the case of the spatially expanded system, Equations (9) and (10) transform into the partial differential Equations (11) and (12),

$$C\frac{\partial\phi_{DL}}{\partial t}=-nFck(\phi_{DL})-\sigma\left.\frac{\partial\phi}{\partial z}\right|_{z=\mathrm{WE}} \tag{11}$$

$$\frac{\partial c}{\partial t}=-\frac{2}{\delta}ck(\phi_{DL})+\frac{2D}{\delta^2}(c_b-c) \tag{12}$$

respectively.[8] The diffusion parallel to the electrode is much slower than all other processes and is therefore often neglected. The migration currents, the last term of Equation (11), at the electrode can be determined if the potential distribution in the electrolyte is known. The potential distribution obeys Laplace's Equation (3) in good approximation. The negative global coupling discussed in Section 3.2 comes into play as a result of the control condition [Eq. (7)] if $z=\mathrm{RE}$ and is between $z=\mathrm{CE}$ and $z=\mathrm{WE}$.

Section 4: Homogeneous S-NDR systems have the structure described by Equations (13) and (14), where $f(u,\phi_{DL})$ is

$$\frac{\mathrm{d}u}{\mathrm{d}t}=f(u,\phi_{DL}) \tag{13}$$

$$C\frac{\mathrm{d}\phi_{DL}}{\mathrm{d}t}=-i_{reac}(u,\phi_{DL})+\frac{U-\phi_{DL}}{RA} \tag{14}$$

bistable in ϕ_{DL} and the reaction current for a given value of u depends monotonically on ϕ_{DL}, for example, exponentially.[38] Together with Equations (3)–(6) and (7) or (8), Equations (15) and (16) describe the dynamic of the spatially expanded system.[38]

$$\frac{\partial u}{\partial t}=f(u,\phi_{DL})+D_u\frac{\partial^2 u}{\partial x^2} \tag{15}$$

$$C\frac{\partial\phi_{DL}}{\partial t}=-i_{reac}(u,\phi_{DL})-\sigma\left.\frac{\partial\phi}{\partial z}\right|_{z=\mathrm{WE}} \tag{16}$$

Symbols used in the equations

A	electrode surface
C	specific double layer capacitance
c_b	bulk concentration of the reacting species
c	concentration of the reacting species in the reaction plane (at $z=\mathrm{WE}$)
D	diffusion constant of the reacting species
D_u	diffusion constant of the autocatalytic species
i_{reac}	reaction current density
I_{tot}	total current through the cell
$k(\phi_{DL})$	rate constant multiplied by a potential-dependent dimensionless term ($k(\phi_{DL})$ shows an N-shaped dependency on ϕ_{DL})
F	Faraday's constant
L	circumference of the ring electrode
n	number of electrons transferred in the electrochemical reaction
R	cell resistance between working and reference electrode
t	time
u	autocatalytic variable (usually concentration or coverage)
U	externally applied voltage for potentiostatic control
x	spatial coordinate parallel to the working electrode
z	spatial coordinate perpendicular to the working electrode
z	(=WE/RE/CE) z position of working, reference, or counter electrode, respectively
δ	thickness of the Nernst diffusion layer
ϕ	potential in the electrolyte
ϕ_{DL}	potential drop across the double layer
ϕ^0	potential distribution at the WE at time $t=0$
σ	specific conductivity of the electrolyte.

We thank Professor Dr. G. Ertl for supporting our work, Dr. J. Oslonovitch for the critical reading of our manuscript, Y. J. Li for help with some figures, and I Reinhardt for proofreading. This work has been partially supported by the DFG in the frame of Sfb 555 and the Fonds der Chemischen Industrie.

Received: May 10, 2000 [A 412]
translated by Dr. Angelika Hofmann

[1] These "strange appearances" refer to the spontaneous occurrence of oscillations in the reaction rate during the oxidation of chromium (W. Ostwald, *Z. Phys. Chem.* **1900**, *35*, 33–76).

[2] I. Prigogine, *Self-Organisation in Non-Equilibrium Systems*, Wiley, New York, **1977**.

[3] Y. E. Volodin, V. V. Barelko, A. G. Merzhanov, *Sov. J. Chem. Phys.* **1982**, *5*, 1146–1159.

[4] G. Philippou, D. Luss, *Chem. Eng. Sci.* **1993**, *48*, 2313 – 2323.
[5] M. G. T. Fechner, *Schweigger J. Chem. Phys.* **1828**, *53*, 129 – 151.
[6] J. L. Hudson, T. T. Tsotsis, *Chem. Eng. Sci.* **1994**, *49*, 1493 – 1572.
[7] M. T. M. Koper in *Advances in Chemical Physics*, *Vol. 92* (Eds.: I. Prigogine, S. A. Rice), Wiley, New York, **1996**, pp. 161 – 296.
[8] K. Krischer in *Modern Aspects of Electrochemistry*; *Vol. 32* (Eds.: B. E. Conway, J. O. Bockris, R. White), Kluwer, New York, **1999**, pp. 1 – 142.
[9] H. L. Heathcote, *Z. Phys. Chem.* **1901**, *37*, 368 – 373.
[10] R. S. Lillie, *Science* **1918**, *48*, 51 – 60.
[11] M. T. M. Koper, *Electrochim. Acta* **1992**, *37*, 1771 – 1778.
[12] G. Flätgen, K. Krischer, *J. Chem. Phys.* **1995**, *103*, 5428 – 5436.
[13] We do not consider pattern formation arising from electrohydrodynamic convection. In this case, ordered structures arise even if the homogeneous dynamic does not contain an autocatalytic term.
[14] J. D. Murray, *Mathematical Biology*, Springer, Berlin, **1990**.
[15] A. S. Mikhailov, *Foundations of Synergetics I*, Springer, Berlin, **1994**.
[16] I. R. Epstein, J. A. Pojman, *An Introduction to Nonlinear Chemical Dynamics*, Oxford University Press, New York, **1998**.
[17] P. Gray, S. K. Scott, *Chemical Oscillations and Instabilities*, Clarendon, Oxford, **1990**.
[18] A. Wacker, E. Schöll, *J. Appl. Phys.* **1995**, *78*, 7352 – 7357.
[19] R. Larter, *Chem. Rev.* **1990**, *90*, 355 – 381.
[20] A. Frumkin, O. Petrii, N. Nicolaeva-Fedorovich, *Dok. Akad. Nauk. SSSR* **1961**, *136*, 1158.
[21] K. Krischer, M. Lübke, W. Wolf, M. Eiswirth, G. Ertl, *Electrochim. Acta* **1995**, *40*, 69 – 81.
[22] G. Flätgen, K. Krischer, *Phys. Rev. E* **1995**, *51*, 3997 – 4004.
[23] U. F. Franck, *Z. Elektrochem.* **1958**, *62*, 649 – 655.
[24] R. Otterstedt, P. J. Plath, N. I. Jaeger, J. C. Sayer, J. L. Hudson, *Chem. Eng. Sci.* **1996**, *51*, 1747 – 1756.
[25] R. Baba, Y. Shiomi, S. Nakabayashi, *Chem. Eng. Sci.* **2000**, *55*, 217 – 222.
[26] S. Nakabayashi, R. Baba, Y. Shiomi, *Chem. Phys. Lett.* **1998**, *287*, 632 – 638.
[27] N. Mazouz, G. Flätgen, K. Krischer, *Phys. Rev. E* **1997**, *55*, 2260 – 2266.
[28] M. Meixner, P. Rodin, E. Schöll, A. Wacker, *Eur. Phys. J. B* **2000**, *13*, 157 – 168.
[29] A. Alekseev, S. Bose, P. Rodin, E. Schöll, *Phys. Rev. E* **1998**, *57*, 2640 – 2649.
[30] Many of the corresponding papers are cited in K. Krischer, N. Mazouz, G. Flätgen, *J. Phys. Chem. B* **2000**, *104*, 7545 – 7553.
[31] P. Grauel, J. Christoph, G. Flätgen, K. Krischer, *J. Phys. Chem. B* **1998**, *102*, 10264 – 10271.
[32] J. Christoph, R. D. Otterstedt, M. Eiswirth, N. I. Jaeger, J. L. Hudson, *J. Chem. Phys.* **1999**, *110*, 8614 – 8621.
[33] R. D. Otterstedt, N. I. Jaeger, P. J. Plath, J. L. Hudson, *Chem. Eng. Sci.* **1999**, *54*, 1221 – 1231.
[34] N. Mazouz, G. Flätgen, K. Krischer, I. G. Kevrekidis, *J. Electrochem. Soc.* **1998**, *145*, 2404 – 2411.
[35] J. Christoph, PhD Thesis, FU Berlin, **1999**.
[36] J. Christoph, P. Strasser, M. Eiswirth, G. Ertl, *Science* **1999**, *284*, 291 – 293.
[37] K. Krischer, *J. Electroanal. Chem.* **2001**, in press.
[38] N. Mazouz, K. Krischer, *J. Phys. Chem. B* **2000**, *104*, 6081 – 6090.
[39] M. T. M. Koper, J. H. Sluyters, *J. Electroanal. Chem.* **1994**, *371*, 149 – 159.
[40] M. T. M. Koper, *J. Electroanal. Chem.* **1996**, *409*, 175 – 182.
[41] P. Strasser, M. Lübke, F. Raspel, M. Eiswirth, G. Ertl, *J. Chem. Phys.* **1997**, *107*, 979 – 990.
[42] P. Strasser, M. Eiswirth, G. Ertl, *J. Chem. Phys.* **1997**, *107*, 991 – 1003.
[43] M. T. M. Koper, M. Hachkar, B. Beden, *J. Chem. Soc. Faraday Trans.* **1996**, *92*, 3975 – 3982.
[44] M. Krausa, W. Vielstich, *J. Electroanal. Chem.* **1995**, *399*, 7 – 12.
[45] O. Lev, A. Sheintuch, L. M. Pismen, A. Wolffberg, *J. Phys. Chem.* **1989**, *93*, 1661 – 1666.
[46] O. Lev, A. Wolffberg, A. Sheintuch, L. M. Pismen, *Chem. Eng. Sci.* **1988**, *43*, 1339 – 1353.
[47] J. Ringland, N. Issa, M. Schell, *Phys. Rev. A* **1990**, *41*, 4223 – 4235.
[48] M. T. M. Koper, *Physica D* **1995**, *80*, 72 – 94.
[49] M. T. M. Koper, P. Gaspard, *J. Chem. Phys.* **1992**, *96*, 7797 – 813.
[50] J. P. Joule, *Philos. Mag.* **1844**, *24*, 106 – 115.
[51] J. L. Hudson, J. Tabora, K. Krischer, I. G. Kevrekidis, *Phys. Lett. A* **1993**, *179*, 355 – 363.
[52] J. C. Sayer, J. L. Hudson, *Ind. Eng. Chem. Res.* **1995**, *34*, 3246 – 3251.
[53] Many examples are discussed in the review ref. [8].
[54] The spatial instability in the galvanostatic example discussed below is most likely not linked to the positive global coupling that is intrinsically present under galvanostatic control.
[55] N. Mazouz, K. Krischer, G. Flätgen, G. Ertl, *J. Phys. Chem. B* **1997**, *101*, 2403 – 2410.
[56] I. Krastev, M. T. M. Koper, *Physica A* **1995**, *213*, 199 – 208.
[57] I. Krastev, M. Nikolova, I. Nakada, *Electrochim. Acta* **1989**, *34*, 1219 – 1223.
[58] S. Bandyopadhyay, A. E. Miller, H.-C. Chang, G. Banerjee, V. Yuzhakov, D. F. Yue, R. E. Ricker, J. Jones, J. A. Eastman, E. Baugher, M. Chandrasekhar, *Nanotechnology* **1996**, *7*, 360 – 371.
[59] P. Grauel, K. Krischer, unpublished results.
[60] R. Otterstedt, P. J. Plath, N. I. Jaeger, J. L. Hudson, *Phys. Rev. E* **1996**, *54*, 3744 – 3751.
[61] R. D. Otterstedt, N. I. Jaeger, P. J. Plath, J. L. Hudson, *Phys. Rev. E* **1998**, *58*, 6810 – 6813.
[62] U. Middya, D. Luss, *J. Chem. Phys.* **1994**, *100*, 3568 – 3581.
[63] The nonlinearity of the reaction dynamics can cause minor oscillations of the nodes when the system is further away from the onset of the instability.[35]
[64] P. Strasser, J. Christoph, W.-F. Lin, M. Eiswirth, J. L. Hudson, *J. Phys. Chem. B* **2000**, *104*, 1854 – 1860.
[65] R. D. Otterstedt, P. J. Plath, N. I. Jaeger, J. L. Hudson, *J. Chem. Soc. Faraday Trans.* **1996**, *92*, 2933 – 2939.
[66] M. M. E. Lejay, R. Wiart, *C. R. Acad. Sci. C* **1973**, *277*, 833 – 835.
[67] I. Epelboin, M. Ksouri, E. Lejay, R. Wiart, *Electrochim. Acta* **1975**, *20*, 603 – 605.
[68] A. N. Frumkin, B. B. Damaskin in *Modern Aspects of Electrochemistry*, *Vol. 3* (Eds.: J. O. Bockris, B. E. Conway), Butterworths, London, **1964**, pp. 149 – 223.
[69] *Adsorption of Molecules at Metal Electrodes*, *Vol. 1* (Eds.: J. Lipkowski, P. N. Ross), VCH, Weinheim, **1992**.
[70] A. M. Turing, *Philos. Trans. R. Soc. B* **1952**, *237*, 37 – 72.
[71] V. Castets, E. Dulos, J. Boissonade, P. de Kepper, *Phys. Rev. Lett.* **1990**, *64*, 2953 – 2956.
[72] We denote *tc* as the characteristic time of a transport process if *tc* is the time after which the maximum of an inhomogeneous structure has decayed to e^{-1} of its original value as a result of a transport process (that is, in the absence of a "reaction term").
[73] Y.-J. Li, J. Oslonovitch, N. Mazouz, F. Plenge, K. Krischer, G. Ertl, *Science*, in press.
[74] I. Z. Kiss, W. Wang, J. L. Hudson, *J. Phys. Chem. B* **1999**, *103*, 11433 – 11444.
[75] K. Krischer, N. Mazouz, G. Flätgen, *J. Phys. Chem. B* **2000**, *104*, 7545 – 7553.
[76] M. Schell, F. N. Albahadily, J. Safar, *J. Electroanal. Chem.* **1993**, *353*, 303 – 313.
[77] P. Strasser, PhD Thesis, FU Berlin, **1999**.